Overview about field measurements in rock masses

Author: Prof. Dr. habil. Heinz Konietzky
(TU Bergakademie Freiberg, Geotechnical Institute)

1 Introduction[1]

Geotechnical field measurements are applied to monitor natural slopes, caves etc. as well as geotechnical constructions like tunnels, mines, caverns, man-made slopes etc. Field measurements are conducted during all phases of the geotechnical construction, but also afterwards as monitoring. There are a lot of recommendations and norms in respect to rock mechanical in-situ measurements (e.g. ASTM, DIN or recommendations by DGGT, ISRM, USBR etc.).

The aims of field measurements are manifold:

- Improvement of general understanding of rock mass behaviour
- Assessment of safety / stability
- Confirmation or disproval of expected or predicted rock mass behaviour respectively
- Use for back analysis of numerical models
- Determination of rock mass parameters
- Determination of scale-effects
- Providing data for quality control
- Conservation of evidence
- Compliance of limits

Typical measurement tasks are:

- Subsidence measurements
- In-situ stress measurements
- Pore / joint water pressure measurements
- Inclination measurements
- Convergence / displacement measurements
- In-situ stiffness determination
- In-situ strength determination
- Temperature measurement

[1] :

- *This E-book chapter does not cover geophysical and geodetic measurements, which are also useful and often applied in geotechnical engineering.*
- *Often a temperature correction has to be performed, because some measuring values show significant temperature dependence. This will not be explicitly mentioned in this E-book chapter.*
- *Not included are special in-situ stress measurement systems to determine the in-situ stress state in the rock mass as they are already discussed in the E-book chapter “03 Rock Stresses”.*

The general requirements can be defined as follows:

- Easy installation and handling even under unfavourable conditions
- Robustness, reusability and long life-time
- Appropriate accuracy and sensitivity
- Safe data storage and/or transmission
- Consideration of influencing factors (e.g. temperature, weather conditions, humidity, electromagnetic fields, vibrations, noise etc.)
- Redundancy (especially important for safety relevant monitoring, but also to recognize measurement errors and to correct them)
- Function check and calibration (both it necessary installation, but also during operation)

Starting in 2013 (Golser & Steiner, 2021) several international standards about geotechnical monitoring and instrumentation were issued:

- EN-ISO 18674-1: General rules
- EN-ISO 18674-2: Measurement along a line – Extensometer
- EN-ISO 18674-3: Measurements across a line – Inclinometer
- EN-ISO 18674-4: Measurement of pore water pressure – Piezometer
- EN-ISO 18674-5: Stress change measurement by total pressure cells (TPC)
- In preparation:
    - Settlement measurements by hydraulic level gauges
    - Strain gauges
    - Load cells
    - Geodetic measurements in geotechnical monitoring
    - Vibration measurements

All of them follow the same structure:

- Scope
- Normative references
- Terms
- Symbols
- Measurement equipment
- Installation and carrying out the measurement
- Data processing and evaluation
- Reporting

2 Basics

The basic measurement parameters are:

- Length
- Pressure
- Time
- Mass

Derived parameters are:

- Displacements (vector)
- Deformations (tensor)
- Stresses (tensor)
- Forces (vector)
- Change in angle (scalar)

We have to distinguish between:

- Measurement parameter (German: “Messgröße”): input value for measuring system and
- measured value (German: “Messwert”): output value of measuring system

In general a geotechnical measuring system consists of four parts: sensor, transmitter, indicating instrument and data logger. All measurements contain errors. Measuring error is defined as the difference between the actual value of a quantity and the value obtained by a measurement. These errors can be subdivided into 3 categories:

- Serious measuring error (due to damage, lack of attention etc.),
- Systematic measuring error (due to systematic temperature change, drift, friction, zero offset etc.),
- Random measuring error (due to random temperature change, vibrations, parasitic currents etc.).

Serious measuring errors can and have to be avoided. Systematic errors can and have to be corrected. Random measuring errors have to be taken into account and can be minimized by multiple measurements and statistical evaluation. The following definitions hold:

(1) Absolut error F:

$$F = A - W ,$$

where A is the measured value (actual value) and W is the true value (reference value)

(2) Relative error *f* related to reference value:

$$f = \frac{F}{W} \cdot 100\ \% = \frac{A - W}{W} \cdot 100\ \%$$

(3) Relative error *f* related to actual value:

$$f = \frac{F}{A} \cdot 100\ \% = \frac{A - W}{A} \cdot 100\ \%$$

(4) Relative error f related to maximum value of measuring range A_{max}:

$$f = \frac{F}{A_{max}} \cdot 100\%$$

Systematic measuring errors of devices are given by following expressions:

$$GK = \frac{|F_{Gmax}|}{MB} \cdot 100\ \% \qquad F_{Gmax} = \frac{\pm MB \cdot GK}{100}$$

where:
GK = accuracy class
MB = maximum value of measuring range
F_{Gmax} = maximum absolute error

Resolution is the number of pieces or parts that the output or displayed reading from a sensor or measuring instrument can be broken down into without any instability in the signal or reading.

Accuracy tells us how closely the output or displayed reading from a sensor or measuring instrument matches the real physical value. Accuracy classes are defined as deviation in relation to full-scale deflection.

Nowadays most measuring devices have a digital display. The corresponding **sensitivity** is defined as the quotient between digital step and change in measurement parameter.

Digital resolution is defined by the number of available digits, for instance:

$8\ \text{bit} = 2^8\ \text{digits} = 256\ \text{digits}$

$12\ \text{bit} = 2^{12}\ \text{digits} = 4096\ \text{digits}$

$16\ \text{bit} = 2^{16}\ \text{digits} = 65{,}536\ \text{digits}$

$32\ \text{bit} = 2^{32}\ \text{digits} = 4{,}294{,}967{,}296\ \text{digits}.$

3 Classification

According to chosen criteria geotechnical field measurements can be subdivided into:

- Permanent and temporary measurements
- Stress and strain or force and displacement measurements
- Small-scale and large-scale measurements
- High precision and low precision (indicator) measurements
- Static (single value) or dynamic (time dependent data series) measurements
- Direct measurements (sensor shows results without any transformation) and indirect measurements (sensor values have to be transformed to get the required physical values)

Measuring tools are working on mechanical or electrical or hydraulic or optical basis. Most popular measuring principles are:

- Strain gauge
- Vibrating-element
- Inductive
- Piezoelectric
- Radiometric
- Photoelectric

4 Typical geotechnical measuring systems (selection)

In the following sub-paragraphs a few often used geotechnical measuring systems are presented in more detail.

4.1 Extensometer

Extensometers are used to measure displacements, convergence, settlements, joint movements etc. They are produced as borehole devices or tools, which are installed in openings (tunnels, drifts, shafts, caverns, chambers etc.) between 2 fixation points.

There are different types of extensometers like:

- Rod extensometers
- Bar extensometers
- Tape extensometers
- Wire extensometers
- Magnetic extensometers

Sensitivity of extensometers applied in rocks is in the order of about 0.01 mm/m. Extensometers can be designed either as single-point or multipoint instrument. The measuring principle can be quite different, e.g.: Electro-mechanic, vibrating wire, fibre optic, magnetic. Often, so-called LVDT (**L**inear **V**ariable **D**ifferential **T**ransformer) are used. This sensor is an electro-mechanical transducer, which forms linear motion into a corresponding electrical signal. The principle (see Fig. 4.1.1) is the following: The moving part is a magnetically permeable material (core, blue coloured) which is fixed on a measuring bar (green). The primary winding (A, middle ring) is energized with constant amplitude and frequency and induces a signal into the secondary windings B (outer rings). According to the actual position of the core the induced signals are distorted and can be used to be interpreted as a displacement.

Fig. 4.1.2 shows different typical extensometer types and Fig. 4.1.3 illustrates the principle of a wire extensometer. A typical multi-point extensometer is shown in Fig. 4.1.4 and Fig. 4.1.5 shows the head of an installed extensometer in an underground mine. Fig. 4.1.6 illustrates a typical measurement design for monitoring the deformations in the tunnel crown.

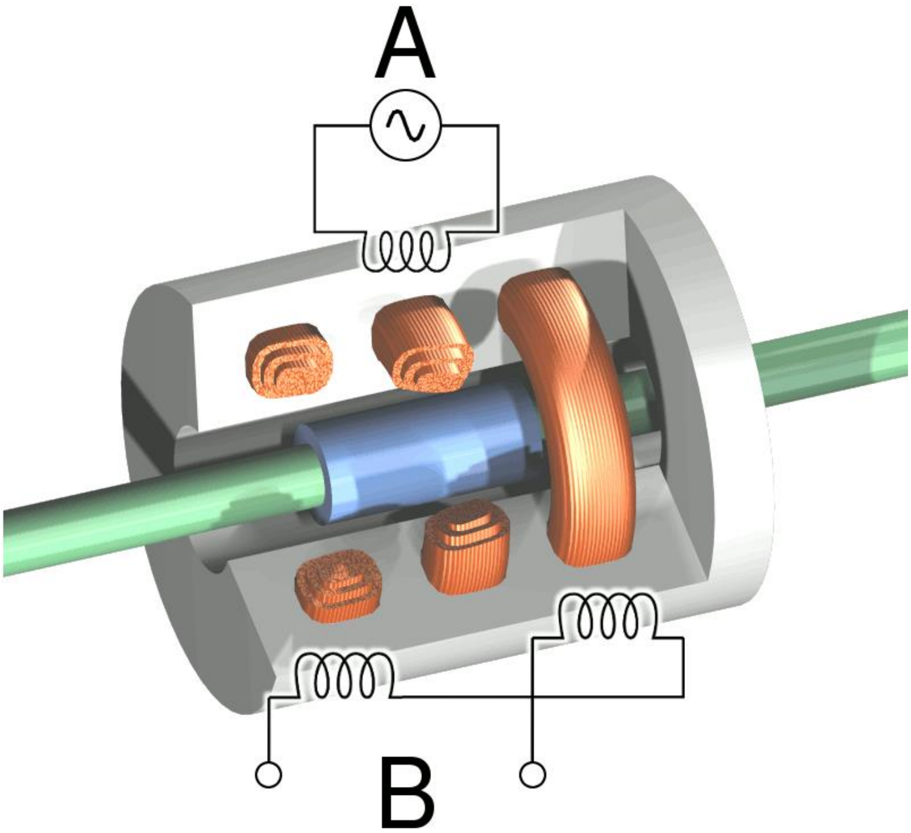

Fig. 4.1.1: Principle of LVDT (https://upload.wikimedia.org/wikipedia/commons/5/57/LVDT.png by Zedh, CC-BY-SA-3.0 [creativecommons.org/licenses/by-sa/3.0, via Wikimedia Commons])

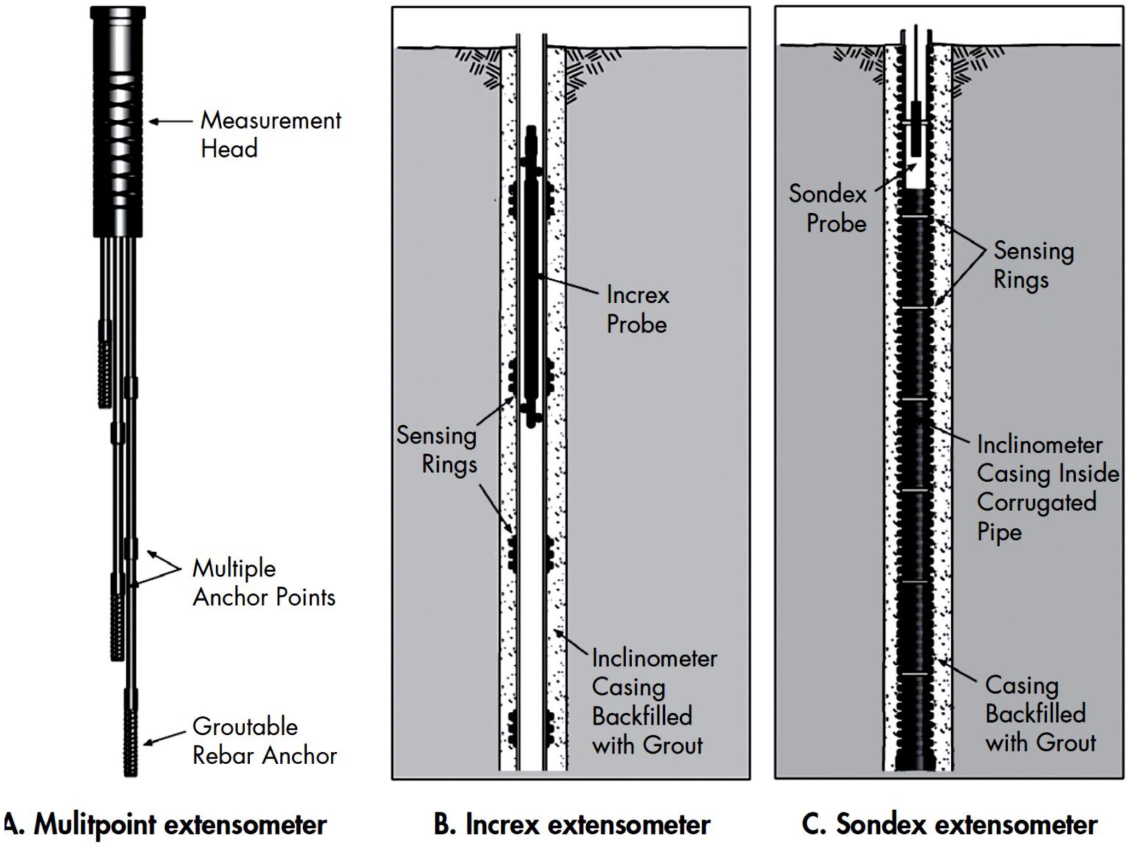

Fig. 4.1.2: Types of borehole rod extensometer (Eberhardt & Stead 2011)

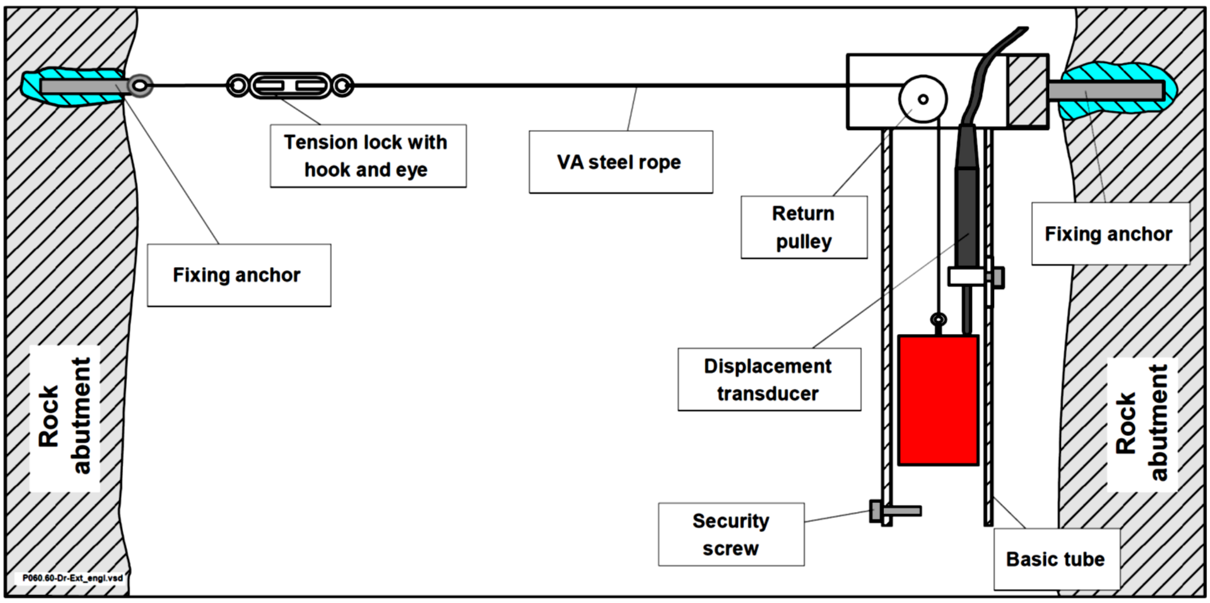

Fig. 4.1.3: Principle of wire extensometer (Glötzl, company material)

Fig. 4.1.4: Typical rod extensometer (Glötzl, company material)

Fig. 4.1.5. Extensometer head (installation in an underground mine)

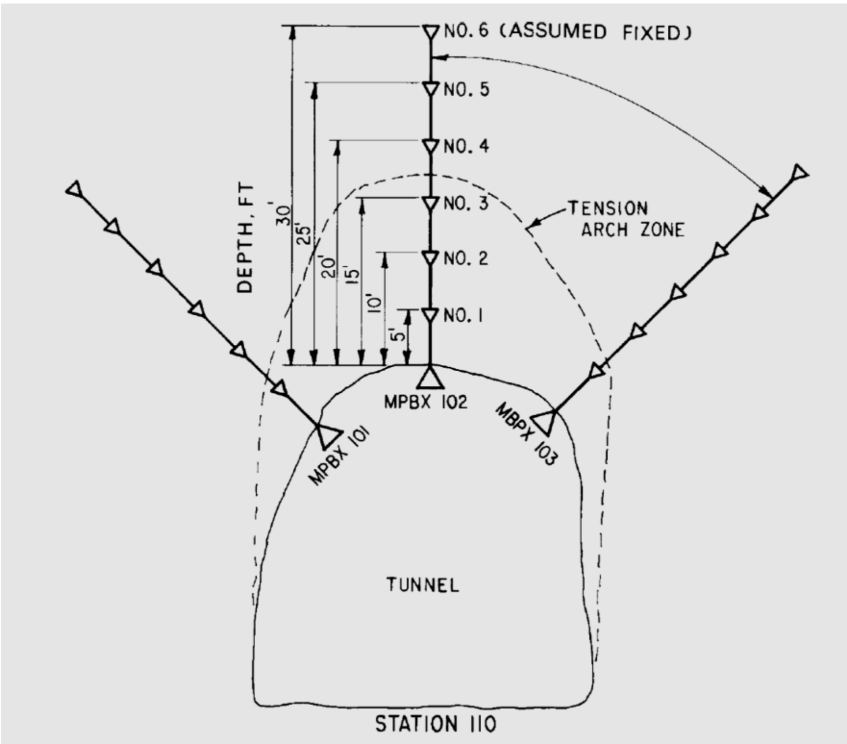

Fig. 4.1.6: Typical multi-point borehole extensometer installation for a tunnel (ASTM 4403-84-2005)

4.2 Digital tape extensometer

Digital tape extensometers (Fig. 4.2.1) are mainly used to measure convergence or deformations inside of tunnels, chambers, caverns or drifts between fixed reference points. Accuracy is up to ± 0.1 mm. Two examples for the typical usage of digital tape extensometers are shown in Fig. 4.2.2 and Fig. 4.2.3.

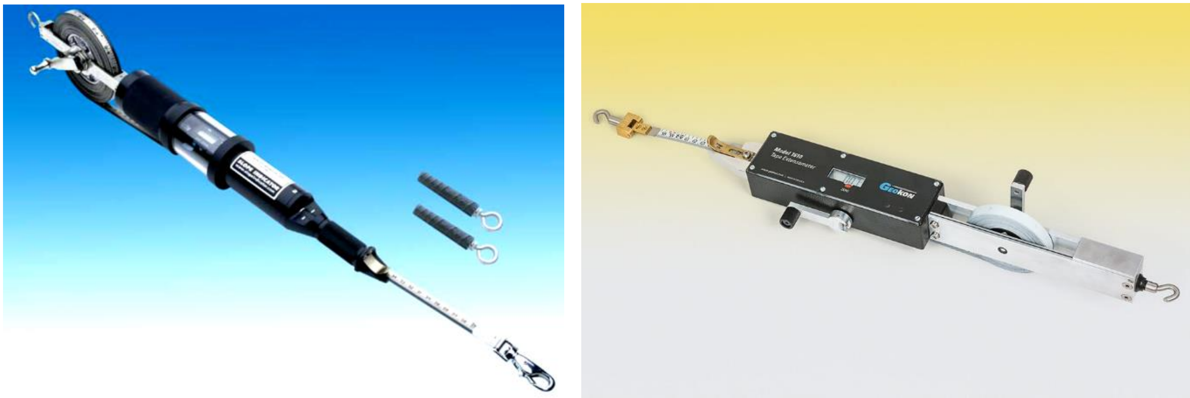

Fig. 4.2.1: Digital tape extensometer (left: Slope Indicator, company material, right: Geokon, company material)

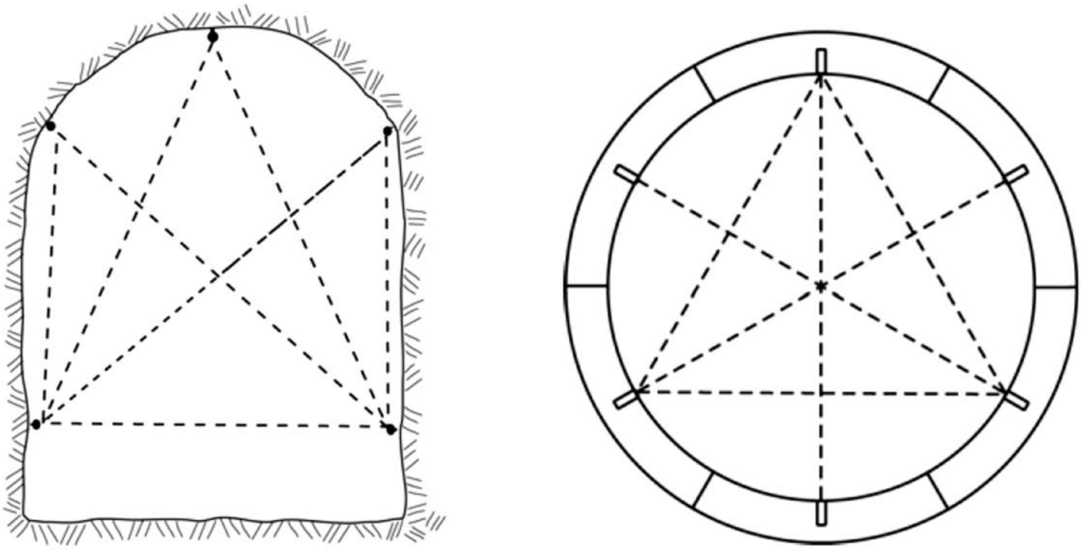

Fig. 4.2.2: Typical measuring profiles for tape extensometers in mining drifts and tunnels

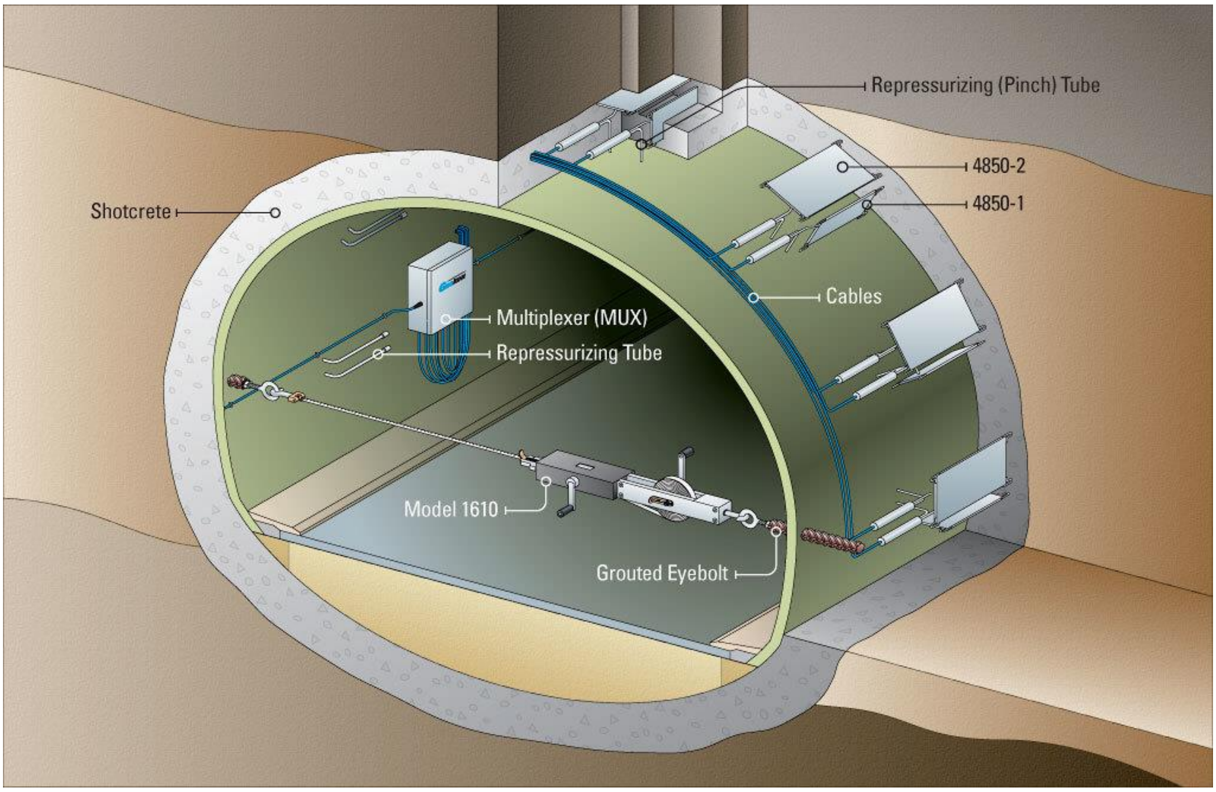

Fig. 4.2.3: Typical installation of tape extensometer in a tunnel (Geokon, company material)

4.3 Inclinometer

Inclinometer are used to measure the inclination of a borehole and consists of two components: The inclinometer casing and the inclinometer measurement system. There are portable and in-place systems. The measuring range is up to about ± 30°. Accuracy is in the order of 0.2 mm/m. Resolution is about 0.005 mm. It is mainly applied to:

- detect shear planes which separate moving horizons (see Fig. 4.3.1),
- monitor settlement profiles when installed horizontally,
- check stability and compliance with design limits.

Exemplary, Fig. 4.3.2 shows a portable inclinometer and Fig. 4.3.3 illustrates the application of an inclinometer in horizontal position. Fig. 4.3.4 shows an application, where an inclinometer is used to verify and monitor a sliding plane of a moving rock mass.

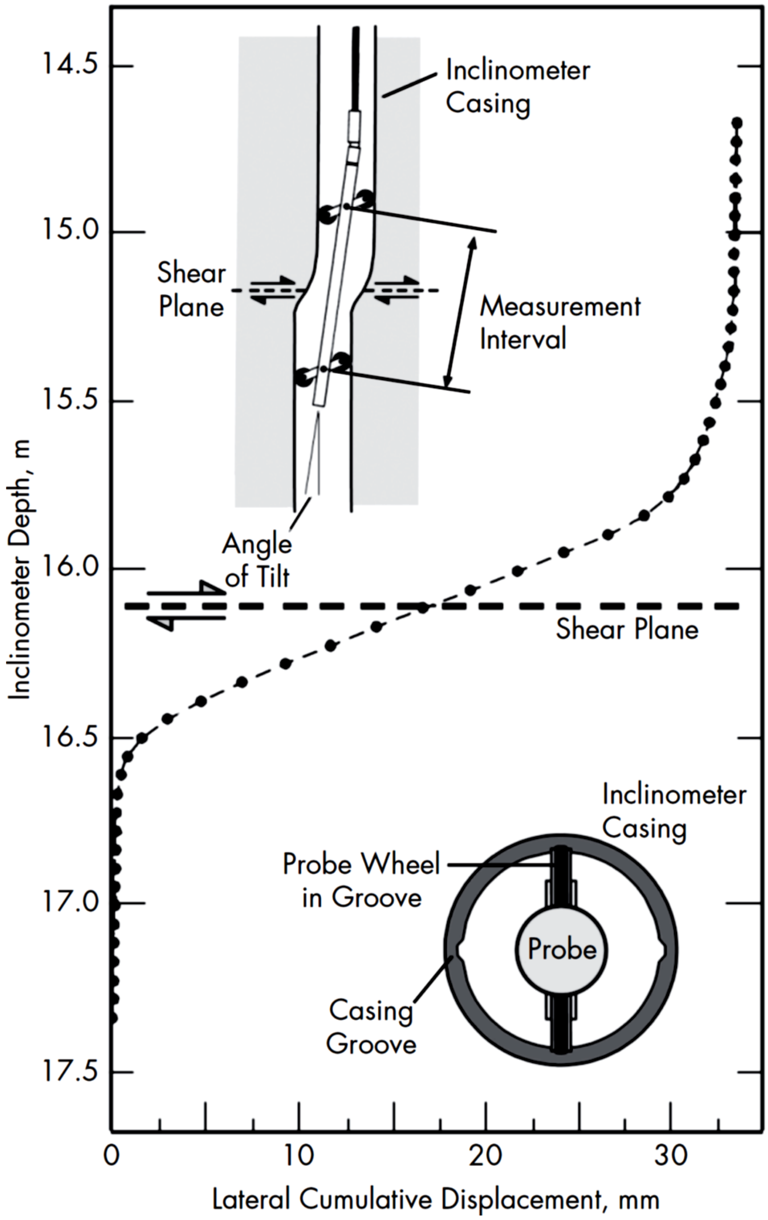

Fig. 4.3.1: Illustration of inclinometer construction and typical measurement result (Eberhardt & Stead, 2011)

Fig. 4.3.2: Portable inclinometer (Slope Indicator, company material)

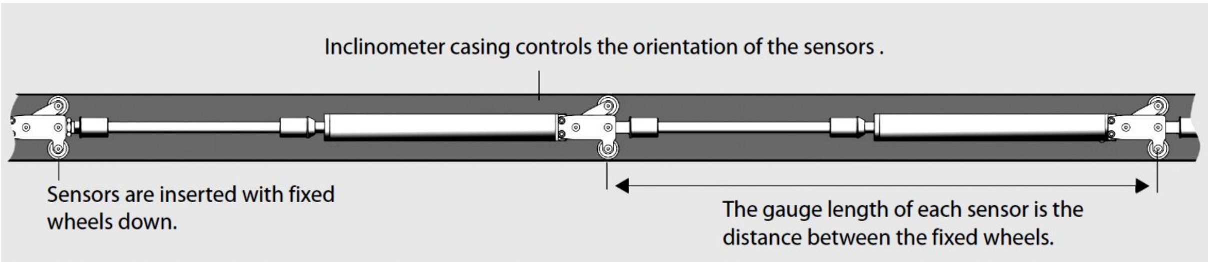

Fig. 4.3.3: Horizontal inclinometer (Slope Indicator, company material)

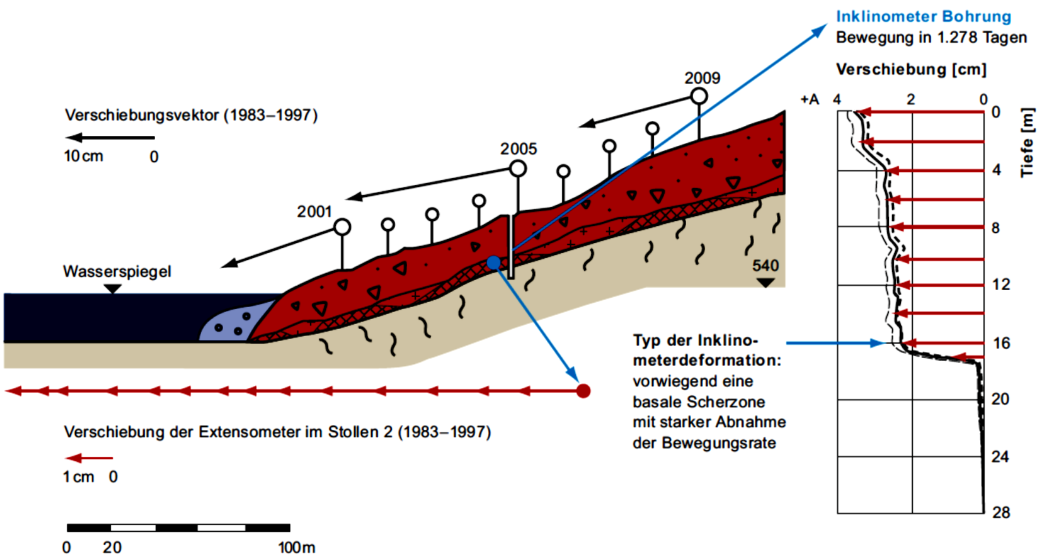

Fig. 4.3.4: Inclinometer measurement results for a sliding rock mass above a stable base rock (Konietzky et al. 2004a, b; Thüringer Fernwasserversorgung 2007)

4.4 Tiltmeter

Tiltmeter (Fig. 4.4.1) can be considered as a special version of inclinometer. Older versions are based on the bubble level principal, but nowadays the microelectromechanical principle (MEMS) measuring in two directions is used. Resolution is in the order of ±0.0005° and measuring range is about ±10°. There are portable or stationary versions.

Fig. 4.4.1: Tiltmeter (Slope Indicator, company material)

4.5 Sliding Micrometer

Sliding Micrometers are installed in boreholes. The measuring principle is illustrated in Fig. 4.5.1. LVDT's deliver the measuring signals. Sliding Micrometers (Li et al. 2013) deliver an accuracy of about ± 0.002 mm/m and the maximum measuring range is 25 mm/m. Common measuring intervals are 1 m. Advanced tools contain also a temperature sensor. Fig. 4.5.2 shows a typical applications using a sliding Micrometer to monitor the development of an excavation disturbed zone (EDZ). Fig. 4.5.3 illustrates the application of sliding micrometers to monitor the deformations of a dam and tunnels.

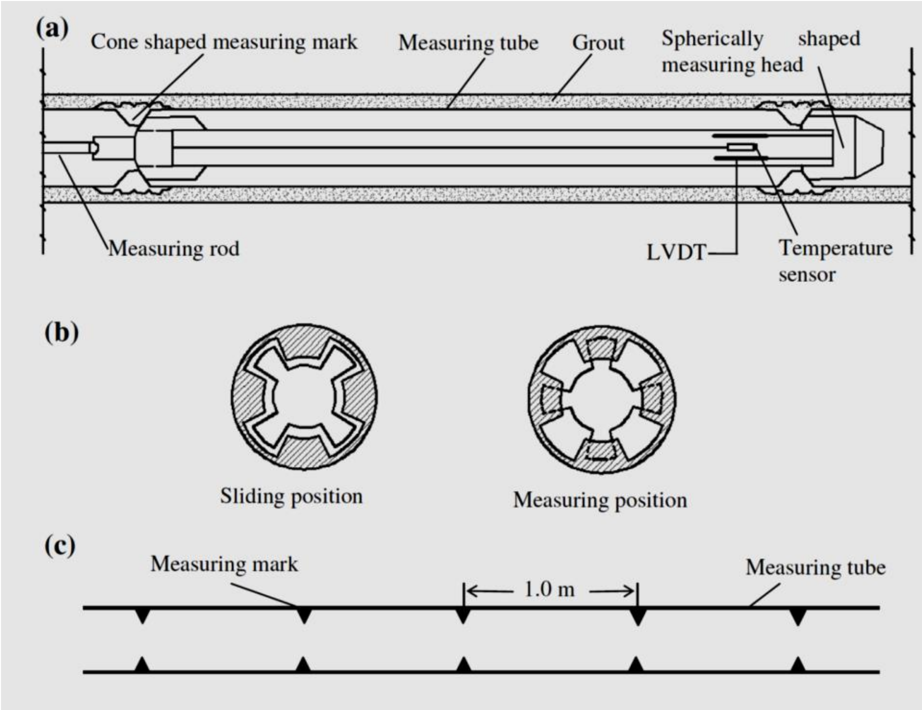

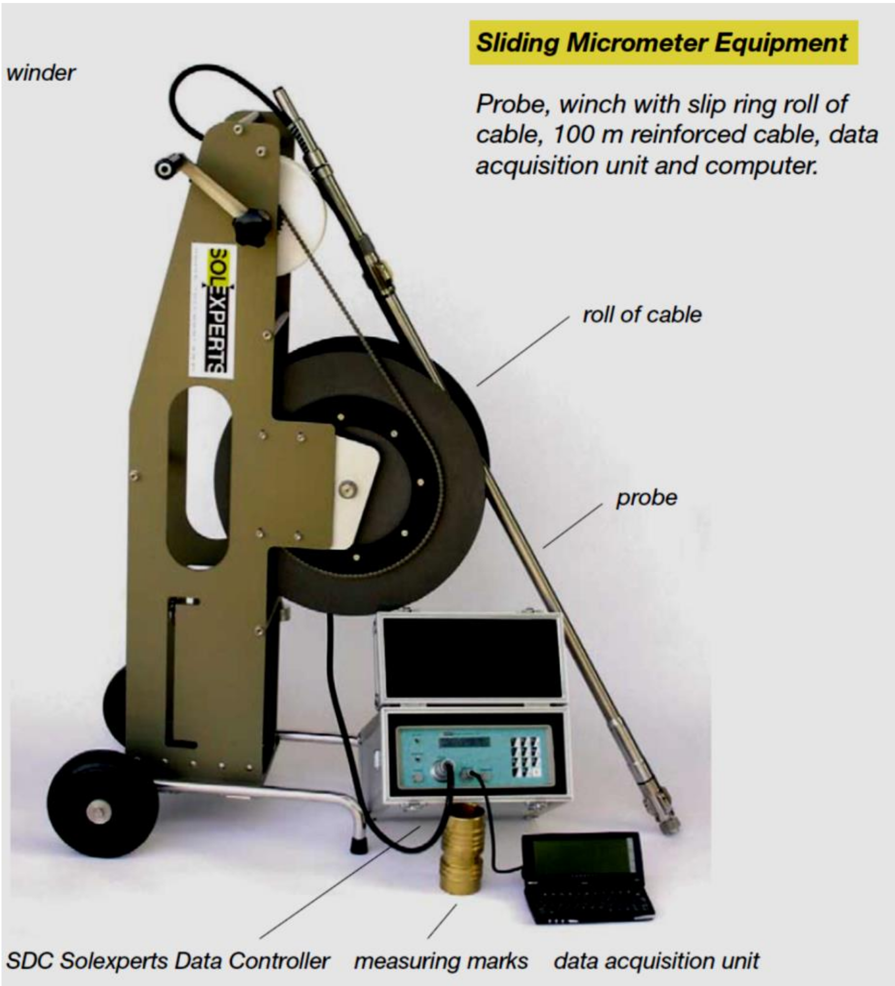

Fig. 4.5.1: Sliding Micrometer: (a) schematic view, (b) sliding and measuring position and (c) interval between measuring marks along the tube (Li et al. 2013) and complete equipment (company material).

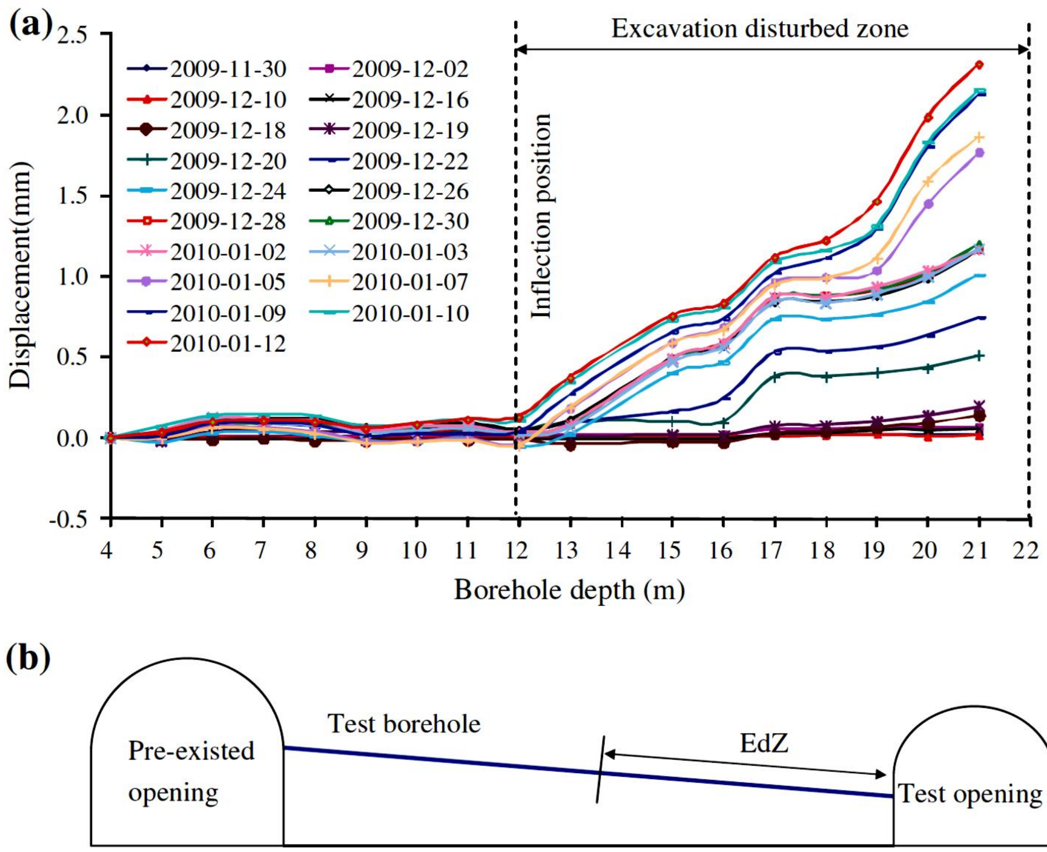

Fig. 4.5.2: Typical measurement results for an excavation disturbed zone (Li et al. 2013)

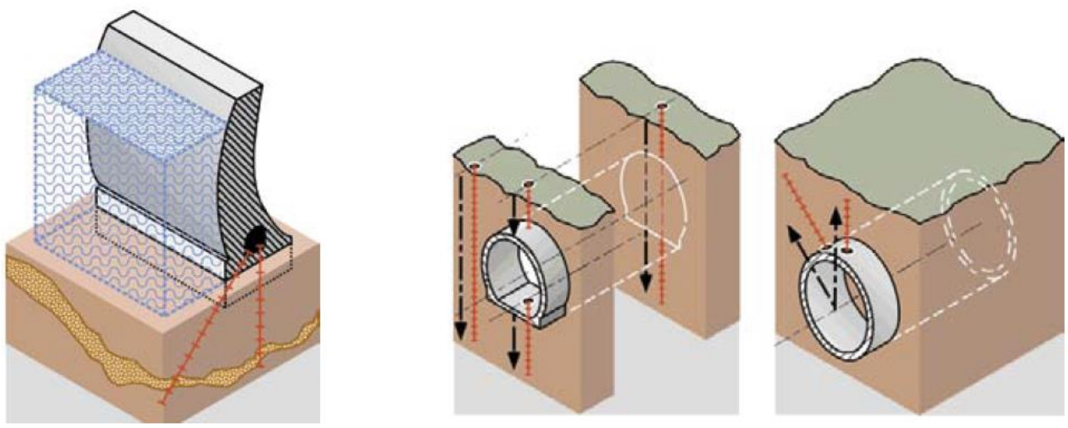

Fig. 4.5.3: Typical applications for sliding micrometers (company material)

4.6 Pressure cells

Pressure cells consist of two stainless steel plates welded together around their periphery and separated by a small gap filled with hydraulic fluid (Fig. 4.6.1). If external pressure is acting on the plates internal fluid pressure is generated. Via a steel tubing the fluid pressure is transmitted to a sensor for recording. Typical accuracy is about 0.1% of maximum value.

Often the vibrating wire system is used, which is based on the following principle: A stretched wire has certain vibrational modes. The half wave length of the fundamental mode is equal to the length of the wire. Assumed there is a magnetic field around the wire: If the frequency of the current in the wire is an eigenmode frequency of wire vibration, it will excite a corresponding harmonic. Strength and phase of excitation depend in field distribution along the wire. Using various frequencies, amplitudes and phases of the resulting vibrations, one can determine corresponding lengthening of the wire (see Fig. 4.6.2).

Paul & Walter (2004) and Franklin (1980) give recommendations for the use of pressure cells in rock engineering, especially for mining and tunnelling. Fig. 4.6.3 shows typical installations of pressure cells to monitor liner stresses in tunnelling. If the 3-dimensional stress state has to be monitored several pressure cells with different orientations have to be applied (see Fig. 4.6.4). Fig. 4.6.5 shows a special pressure cell combination developed to measure radial and tangential stresses in tunnel linings (shotcrete or mass concrete) and Fig. 4.6.6 illustrates typical instrumentation for a tunnel project.

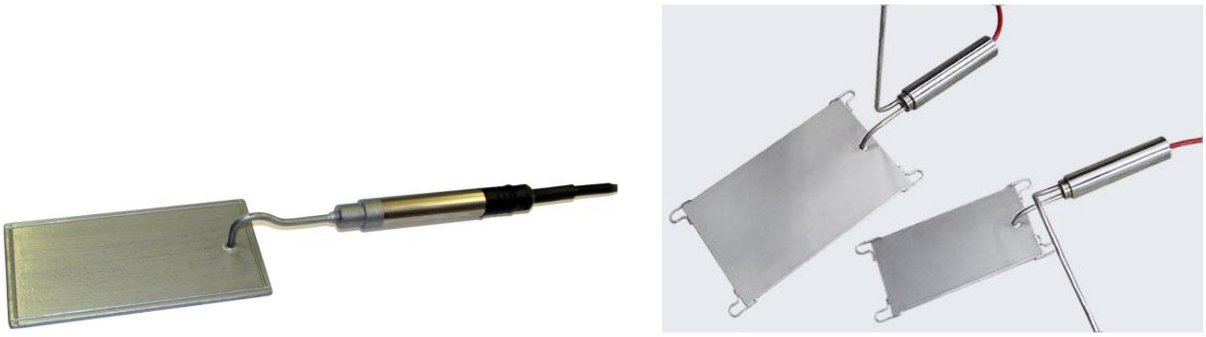

Fig. 4.6.1: Pressure cells (Glötzl, company material)

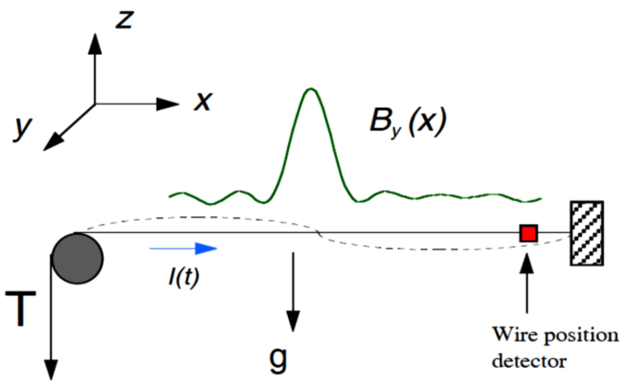

Fig. 4.6.2: Principle of vibration wire system (Temnykh 1997)

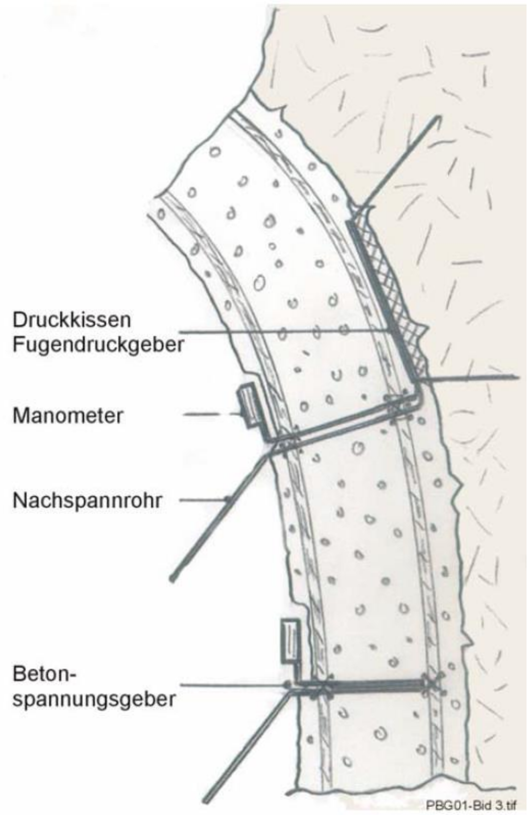

Fig. 4.6.3: Typical installation of pressure cells to monitor liner stresses in tunnels (Glötzl, company material)

Fig. 4.6.4: Stress monitoring station with four pressure cells (Glötzl, company material)

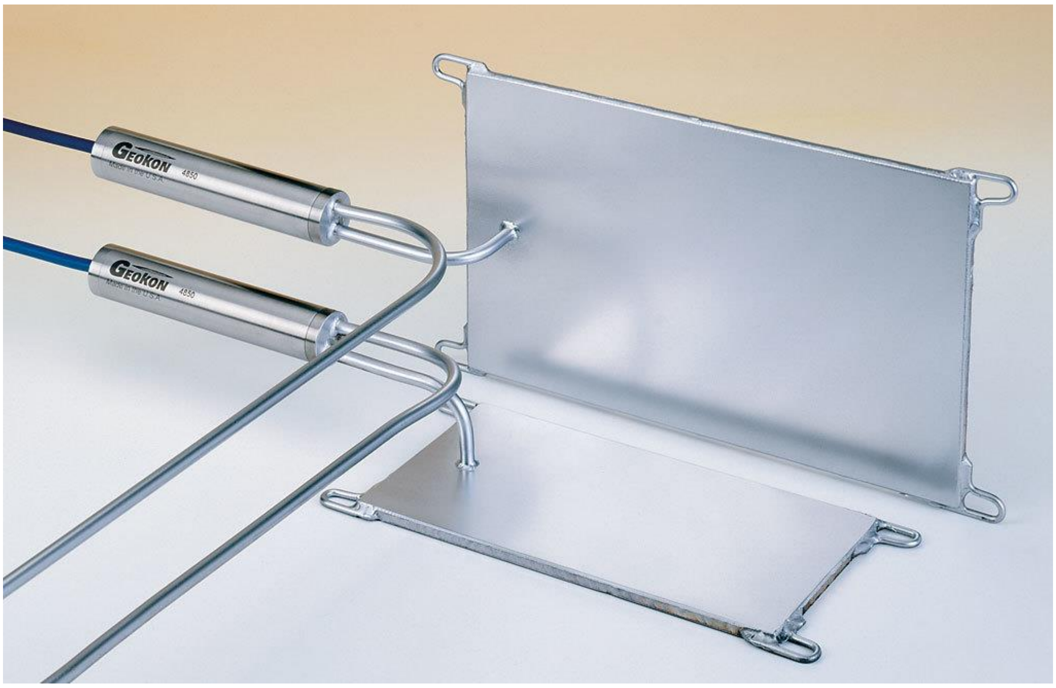

Fig. 4.6.5: Pressure cell combination (Geokon, company material)

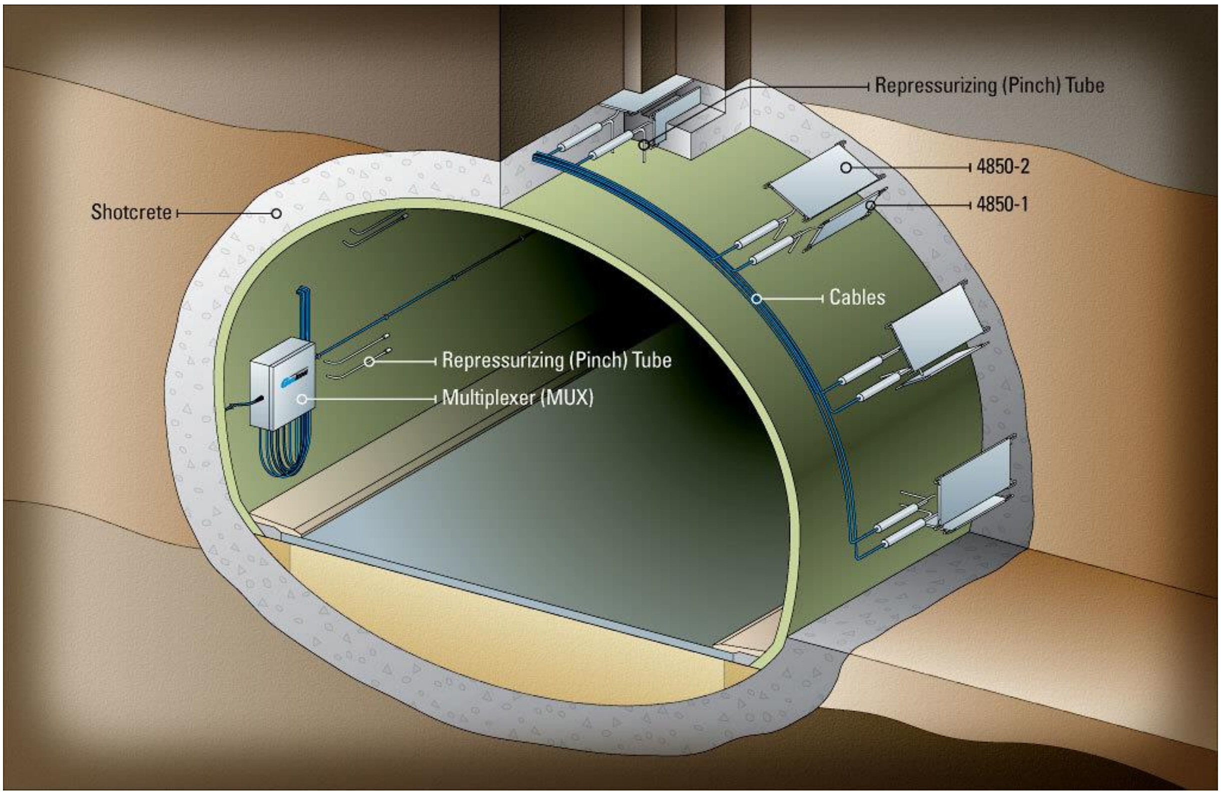

Fig. 4.6.6: Typical installation of pressure cells to monitor stresses in concrete lining (Geokon, company material)

4.7 Crack spy

A crack spy is used to monitor displacements of cracks or fractures in one or two directions (Fig. 4.7.1). Accuracy is about 0.5 mm and typical maximum displacement is in the order a few centimetres. Fig. 4.7.2 shows the application of two crack spies in an underground mine to monitor cracks at the sidewalls of a chamber.

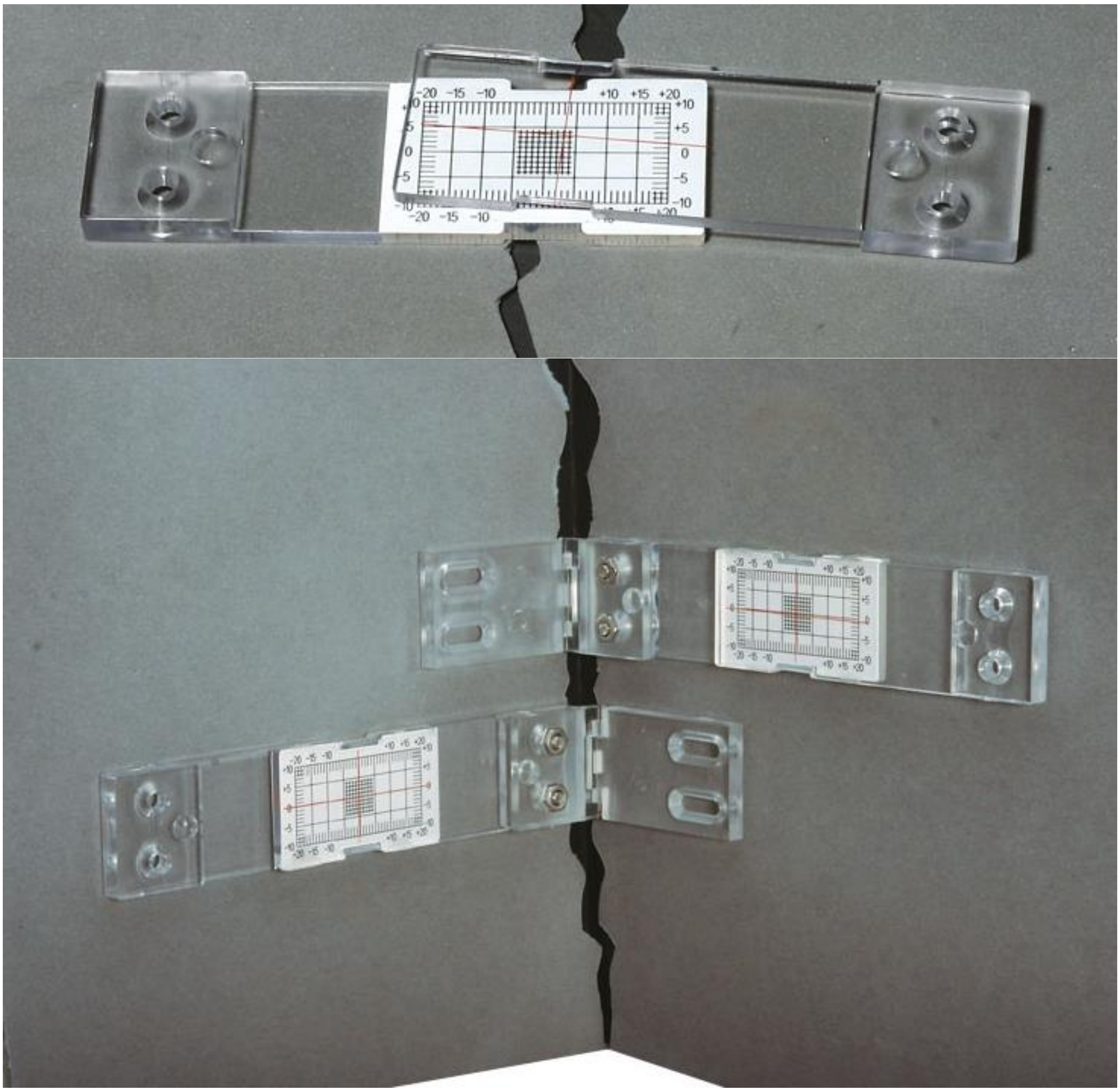

Fig. 4.7.1: Crack spy: above standard tool, below tool for corners (Geocke, company material)

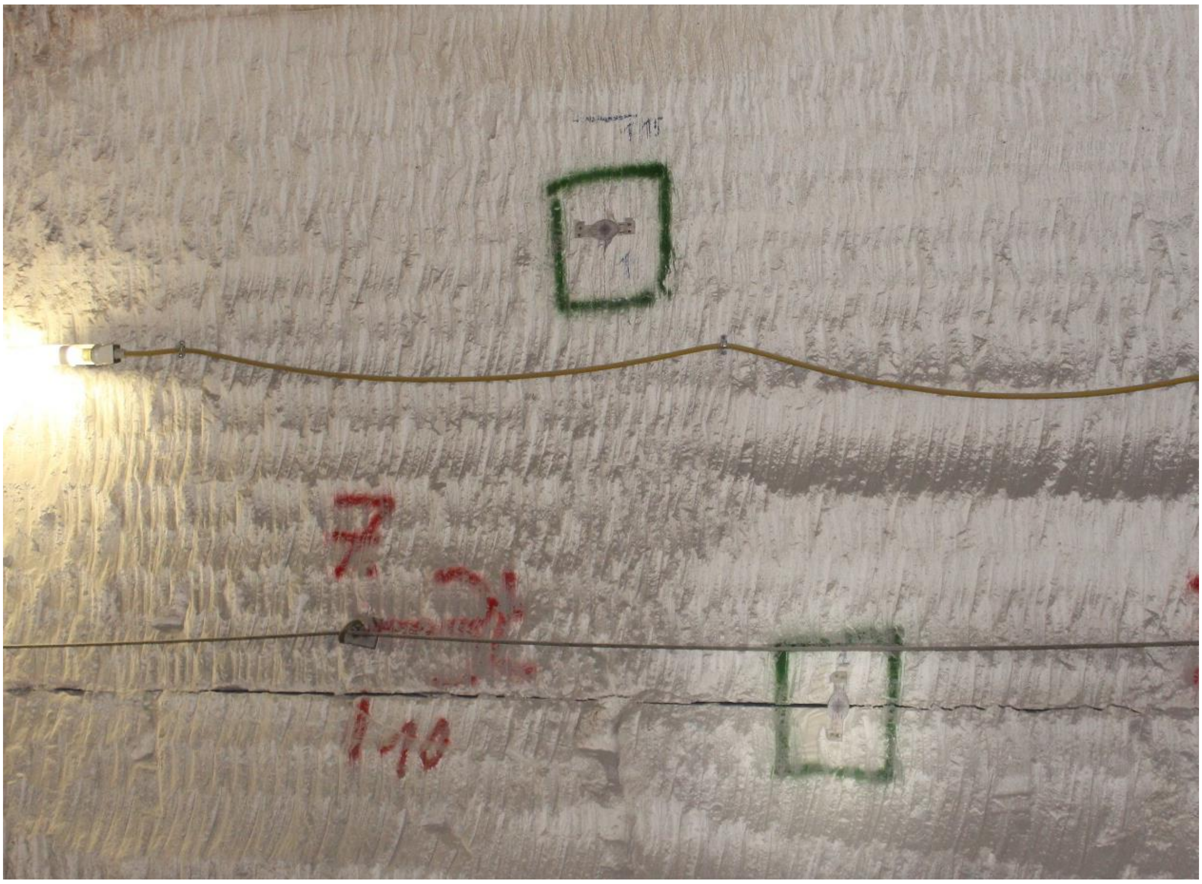

Fig. 4.7.2: Two crack spies (installation in an underground mine)

4.8 Fissurometer / Crackmeter

Fissurometers (also called crackmeters) are high-precision instruments (accuracy between ±0.1 mm and ±0.01 mm) to monitor displacements between two fixation points. Typical length is up to 1 m or slightly longer (Fig. 4.8.1 and 4.8.2).

Typical applications for crackmeters are:

- use as warning system for potential rock fall or collapse of rock engineering structures,
- monitoring of crack behaviour under seismic loading,
- assessment of stability / instability,
- conservation of evidence for constructions.

Crackmeters can be enhanced to measure displacements in all three directions. Fig. 4.8.3 illustrates the measuring principle of a 3D-crackmeter. Janeras et al. (2015) show an interesting complex deformation monitoring in the Montserrat Massif (Spain) including joint monitoring via crackmeters. Fig. 4.8.4 shows a crackmeter installed in an underground mine.

Fig. 4.8.1: Fissurometer (Interfels, company material)

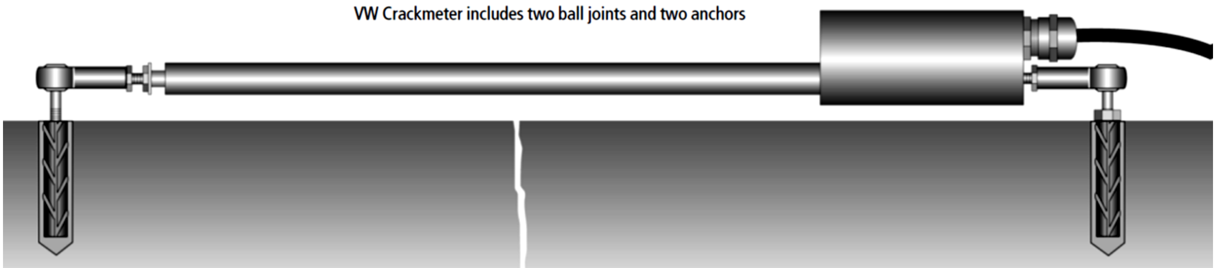

Fig. 4.8.2: Installation of a crackmeter (Slope Indicator, company material)

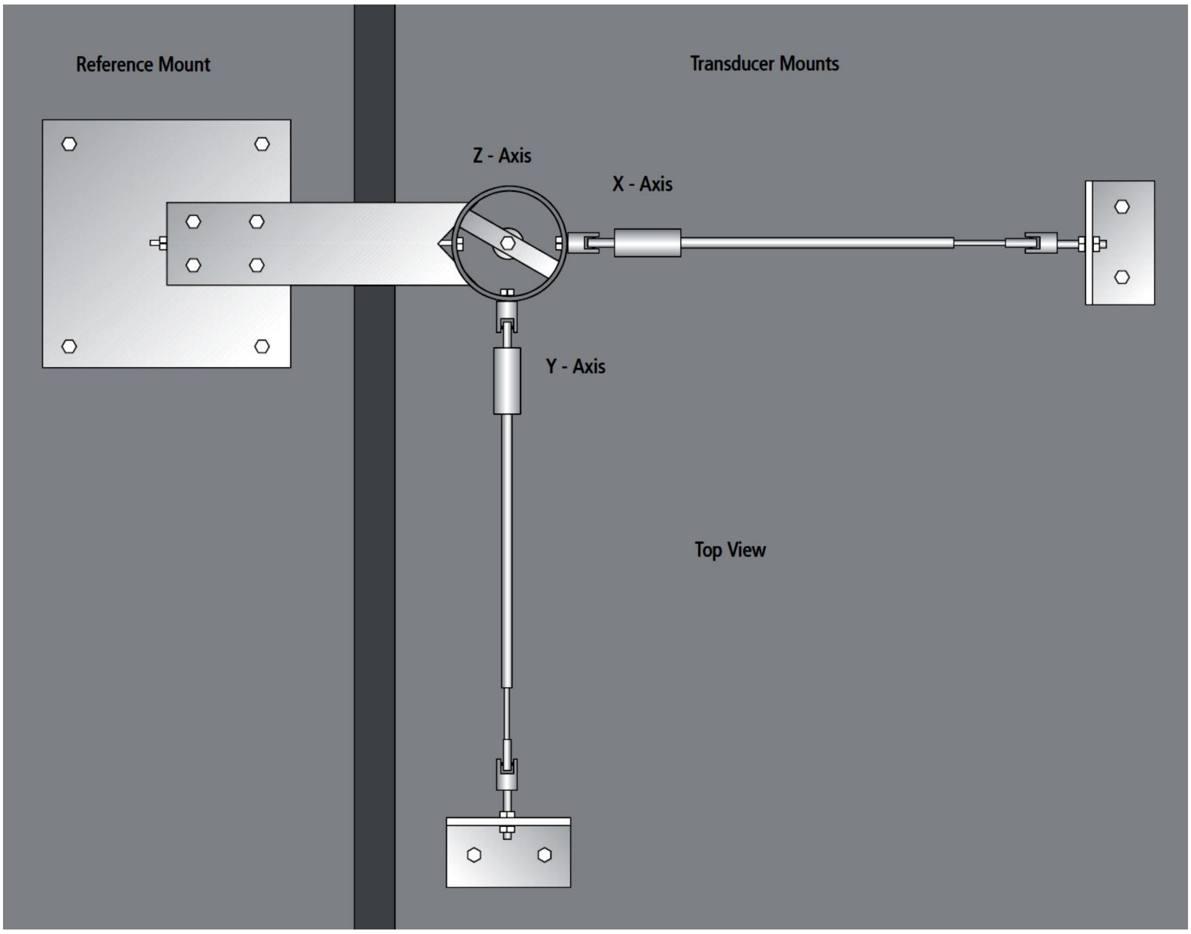

Fig. 4.8.3: 3D-crackmeter (Slope Indicator, company material)

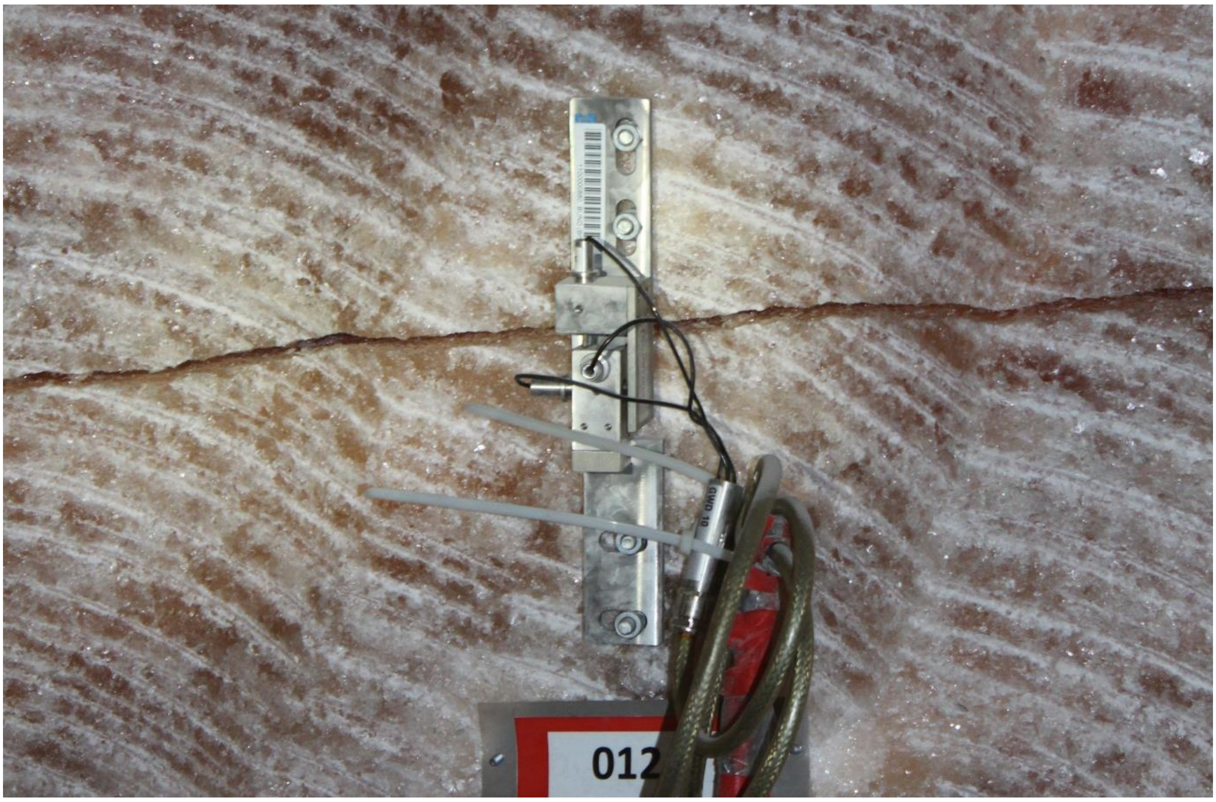

Fig. 4.8.4: Crackmeter (installation in an underground mine)

4.9 Borehole dilatometer

Borehole dilatometers are used to measure the in-situ deformation modulus (stiffness, deformability) of the rock mass. There are two typical constructions:

- Hydraulic cylinders moving shell-type loading plates (Fig. 4.9.1 and 4.9.2)
- Hose packers with either volumetric measurement or displacement transducer to measure of borehole deformability (radial-symmetric loading, see also Fig. 4.9.3).

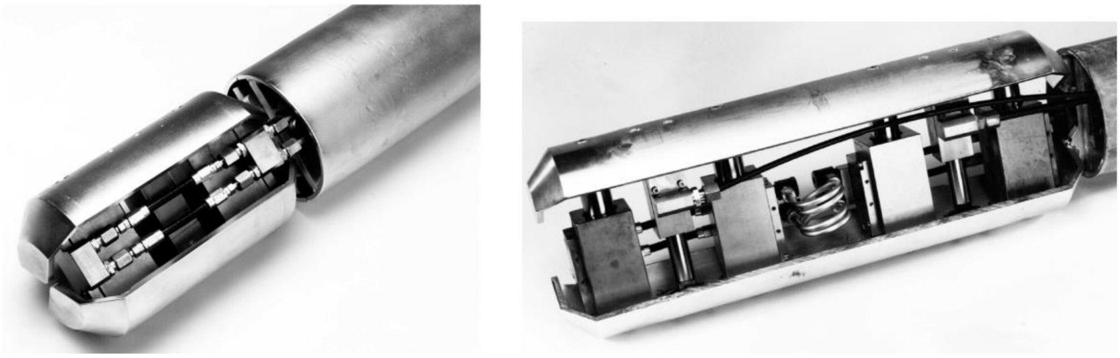

Fig. 4.9.1: Borehole dilatometer with shell-type loading plates (GIF, company material)

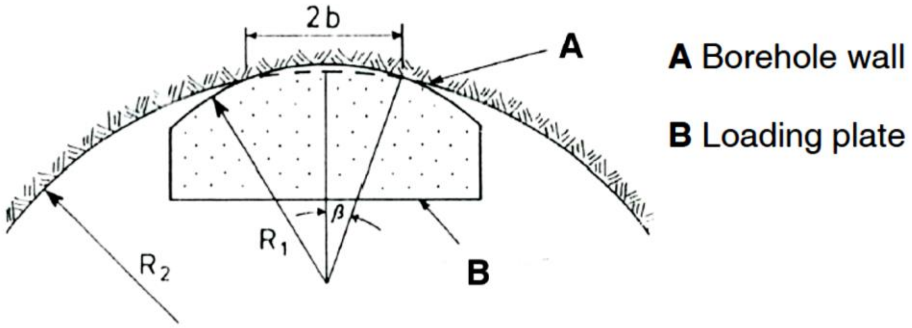

Fig. 4.9.2: Incomplete contact between loading plate and borehole wall (GIF, company material)

A drawback of using loading plates is the incomplete contact between borehole wall and loading plates (see Fig. 31). On the other side this technique allows to apply higher pressure beneficial for stiff rocks. Accuracy of borehole dilatometer can reach about 0.001 mm and displacements of several mm. Based on measured stress and deformation the in-situ deformation modulus can be estimated using analytical solutions based on theory of elasticity.

Goodman (1968), Zelasky et al. (2007) and Yow (2014) give general recommendations for using borehole dilatometers in rock engineering. Special designed dilatometers where pressure is applied only over a small area can be used to determine the stiffness anisotropy just by rotation of the tool or the separate activation of stamps in different direction.

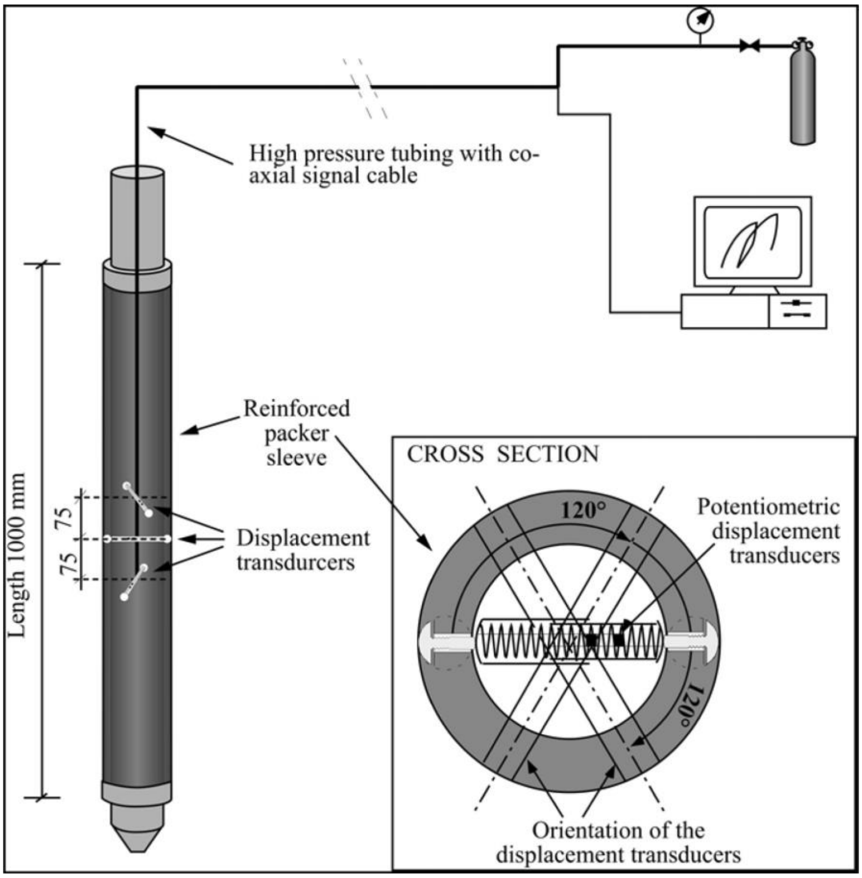

Fig. 4.9.3: Principle of hose packer type dilatometer (Zalesky et al. 2007)

4.10 Loading plates

Loading plates are mainly used to conduct either so-called plate loading tests or in-situ shear tests. Plate loading tests (Fig. 4.10.1) are used to determine the deformability of the rock mass at a larger scale. Therefore, the size of the loading plates are big, so that also fractures or joints etc. are encompassed by the measurement. For counter bearing often the rock mass itself is used, sometimes anchorage is applied in addition. Large hydraulic forces are necessary to produce the desired displacements. The key components are: hydraulic cylinder to generate compressional force including a pressure cell to monitor the applied stress, loading platens to transmit the force to the rock mass and to generate a counter bearing as well as deformation measuring tools (e.g. extensometer).

Practical applications including date interpretation are given for instance by Aghaziri et al. (2012) and Kuvur et al. (2015). Fig. 4.10.2 illustrates the tremendous influence of existence, orientation and density of fractures on the stiffness of the rock mass. In ISRM (1979) and ASTM (2008) general testing procedure and evaluation are described.

In-situ shear tests are performed to determine peak and residual shear strength of the rock mass (rock matrix or joints). By measuring normal and shear forces as well as normal and shear displacements at different normal stress the complete failure envelope can be constructed and friction and cohesion can be determined. Fig. 4.10.3 shows a typical set-up. Using multi-stage technology the shear failure envelope can be constructed with only one test set-up.

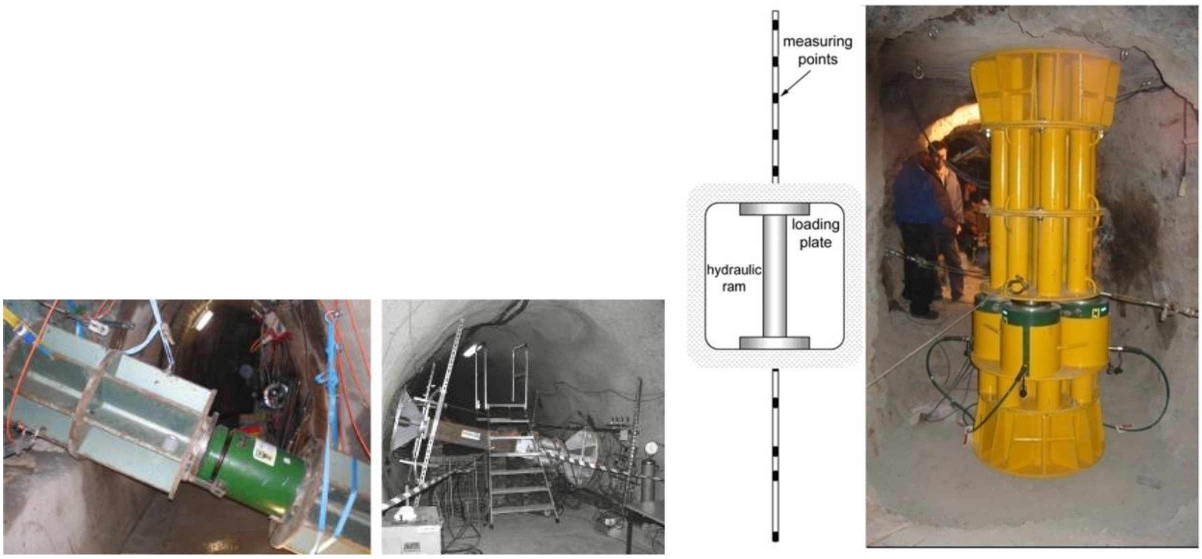

Fig. 4.10.1: Plate loading test set-up in a drift (left: Solexperts, company material; right: Aghaziri et al. 2012)

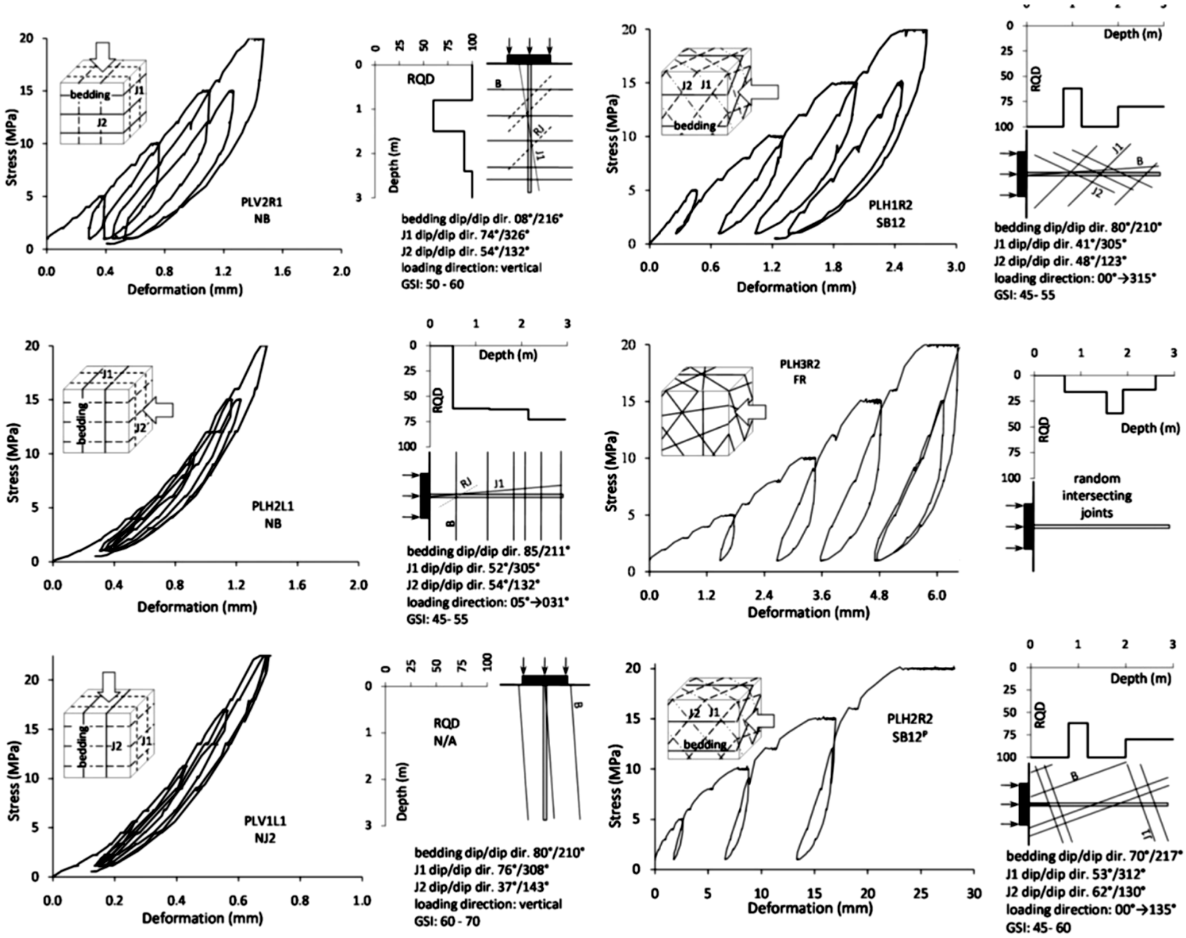

Fig. 4.10.2: Stress-deformation curves of plate loading test with different orientation to fracture system (Aghaziri et al. 2012)

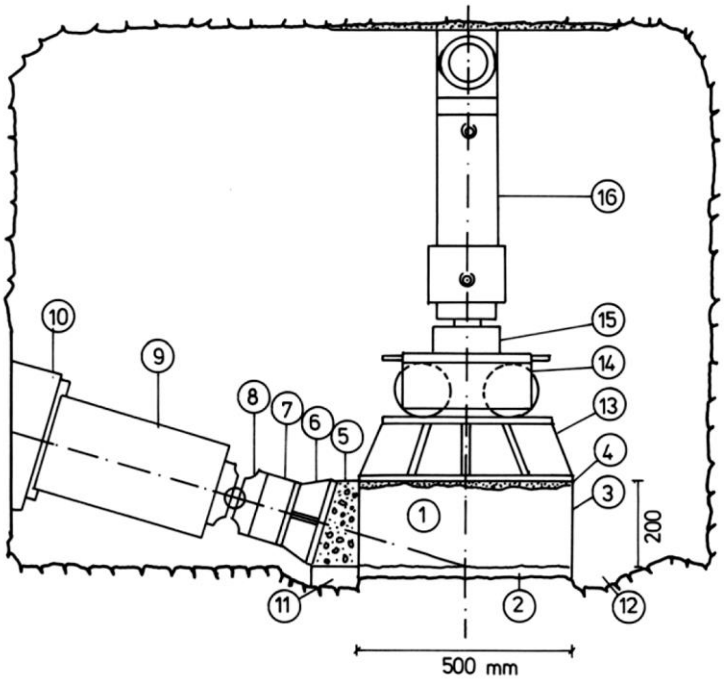

Fig. 1 In-situ shear test on a specimen of 500 x 500 x 200 mm or 1000 x 1000 x 300 mm

1 Test block
2 Shear joint
3 Jacket made of steel sheet
4 Levelling mortar
5 Abutment
6 Load distribution plate
7 Load cell
8 Ball joint
9 Jack for 1 MN
10 Abutment
11 Styrene
12 Drainage ditch
13 Load distribution plate
14 Roller bearing
15 Load cell
16 Jack for 0.2 MN or 1 MN

Fig. 4.10.3: Typical set-up for in-situ shear test (GIF, company material)

4.11 Stressmeter

Stressmeters record compressive stress changes. They are applied in rock masses, concrete or even ice. Exemplary, Fig. 4.11.1 shows a biaxial stressmeter based on the vibrating wire technique. Stressmeters are delivered for certain stress levels. Accuracy is about 0.1 % of maximum value. Stresses are measured perpendicular to the sensor axis. The stressmeter has to be grouted in the borehole. The cylindrical steel cover of the stressmeter will deform under pressure change and induce a sensor signal.

Fig. 4.11.1: Biaxial stressmeter, right: cross section with wire system (Geokon, company material)

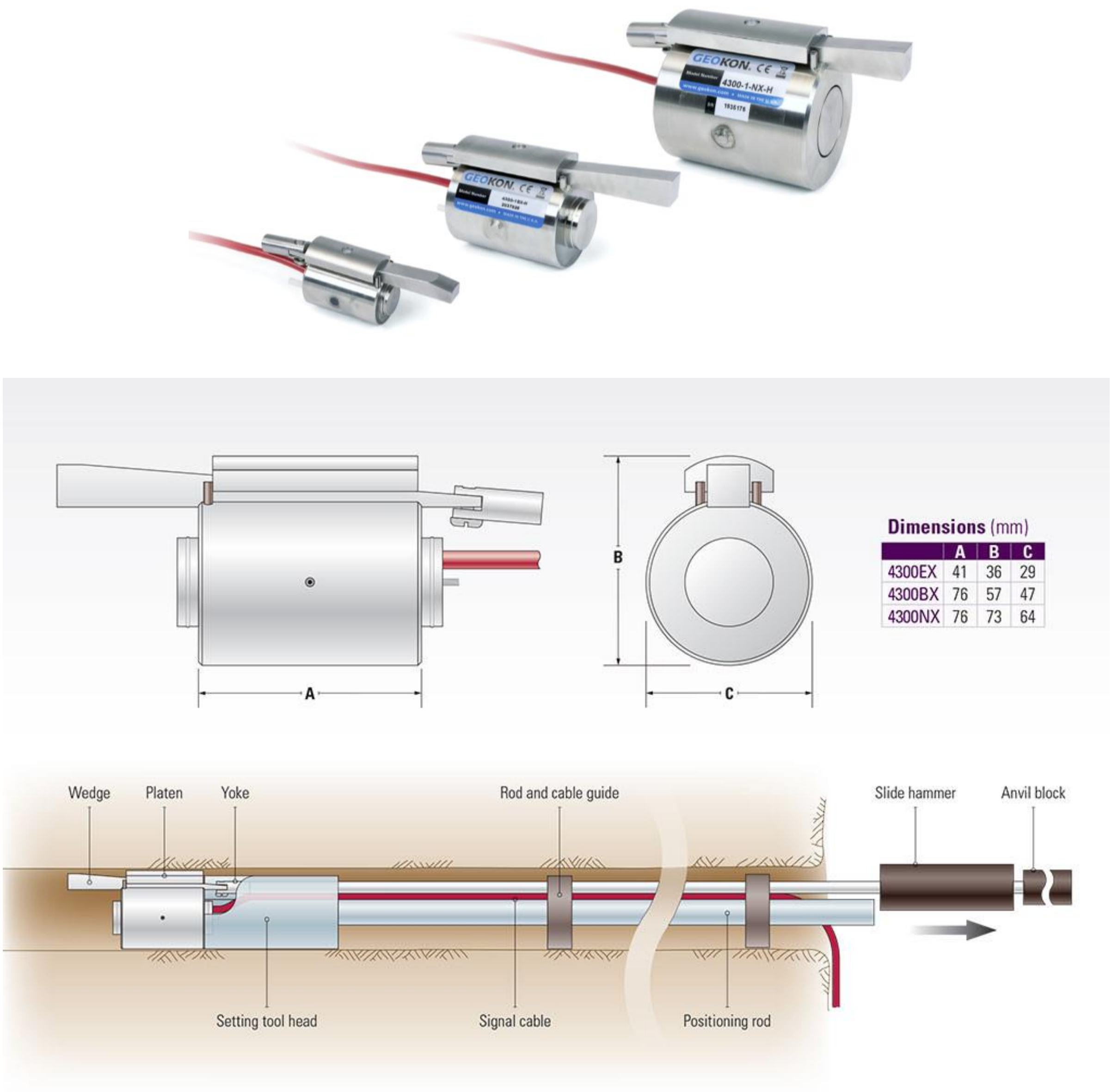

Fig. 4.11.2: Stressmeter for different borehole diameter (Geokon, company material)

The stressmeter is fixed via a wedge to the borehole wall and allows to measure stress changes perpendicular to the borehole wall. Fig. 4.11.3 illustrate the different parts of the tool and the installation procedure. Installation is possible up to a borehole depth of about 30 m.

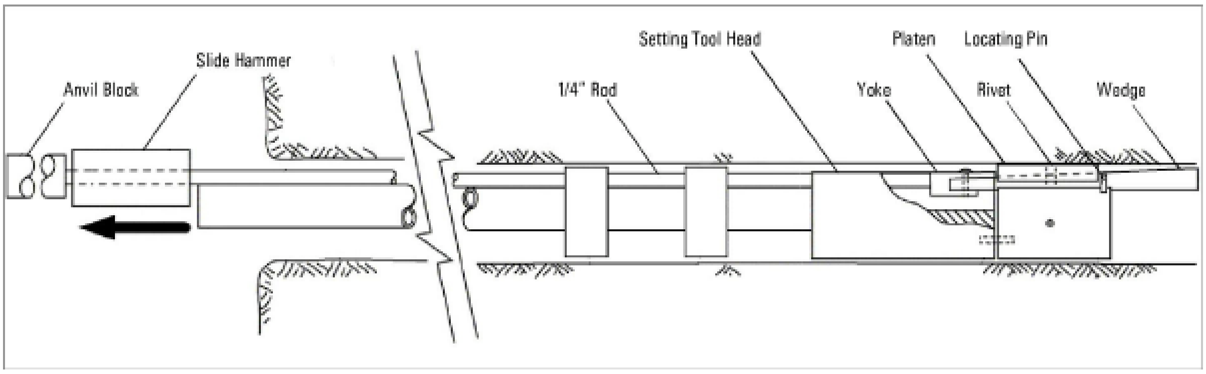

Fig. 4.11.3: Installation procedure for stressmeter into a borehole (Geokon, company material)

4.12 Piezometer

Piezometers (Fig. 4.12.1 and 4.12.2) are used to measure water pressure in soils or rock masses. Typically they are installed in boreholes. Standpipe piezometers are used to monitor water pressure over longer time spans, short-term changes of water pressure are better recorded by diaphragm piezometers (Wyllie 2017). Typical accuracy is 0.1 %. Piezometers are delivered for quite different pressure ranges up to several tens of MPa. Multi-level piezometers have several sensors connected to one communication channel and allow to monitor water pressures at different locations (depths). Important in that case is the isolation of measuring intervals by grouting.

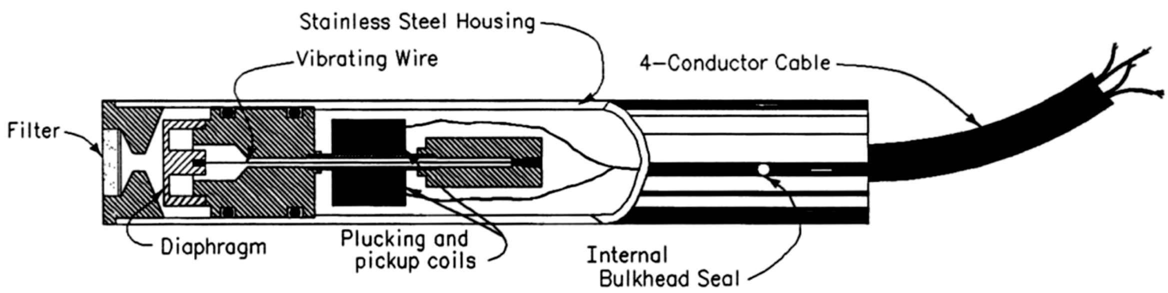

Fig. 4.12.1: Principle of vibration wire piezometer (USBR 2009)

Fig. 4.12.2: Typical piezometers (Roctest, company material)

4.13 Fibre optical measurement devices

In general, fibre optical measurement equipment consists of the following components:

- light source: lasers or LEDs,
- photodetectors
- optical fibres
- optical amplifiers and modulators

Fibre optical systems couple light into glass fibres and analyse the backscattered light. Depending on the measurement principle, either wavelength, intensity or frequency are measured. The accuracy is in the order of 1 µm/m measuring length (similar to DMS). Fibre optical systems have already seen broad applications in rock mechanics, for instance:

- long-term monitoring of deformations in tunnel linings (e.g. Henzinger et al. 2018),
- anchor force monitoring (e.g. Liang & Fang, 2018),
- monitoring of crack movements (Moore et al., 2010),
- monitoring rock mass deformation in mining (e.g. Tang & Cheng, 2018).
- monitoring of deformation of masonry walls (e.g. Wu et al., 2022)

The most common technique used in geotechnics is the so-called Fibre Bragg Grating (FBG), which allows to measure temperatures and strains (often both physical values are measured in parallel to perform temperature compensation). The measured strains can also be used to deduce stress changes, like illustrated by Henzinger et al. (2018). The FBG technology is based on the installation of several reflection points of equal distance inside an optical fibre. If this fibre is stretched, the reflection and refraction pattern changes and can be evaluated as strain (Fig. 4.13.1). Three practical applications are illustrated in Fig. 4.13.2 to 4.13.4.

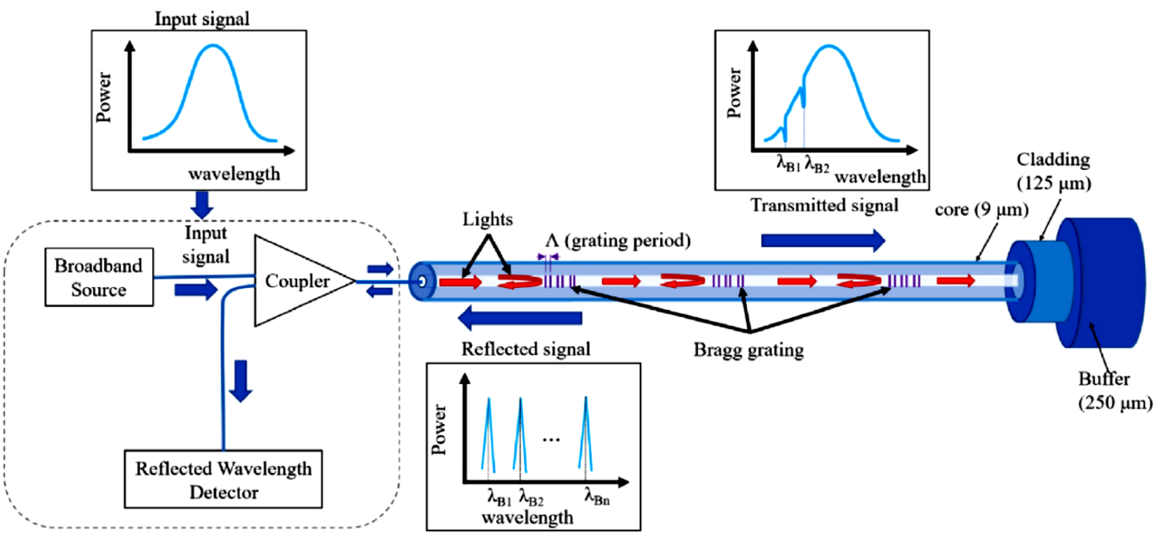

Fig. 4.13.1: Illustration of Fibre Bragg Grating principle (Wu et al., 2022)

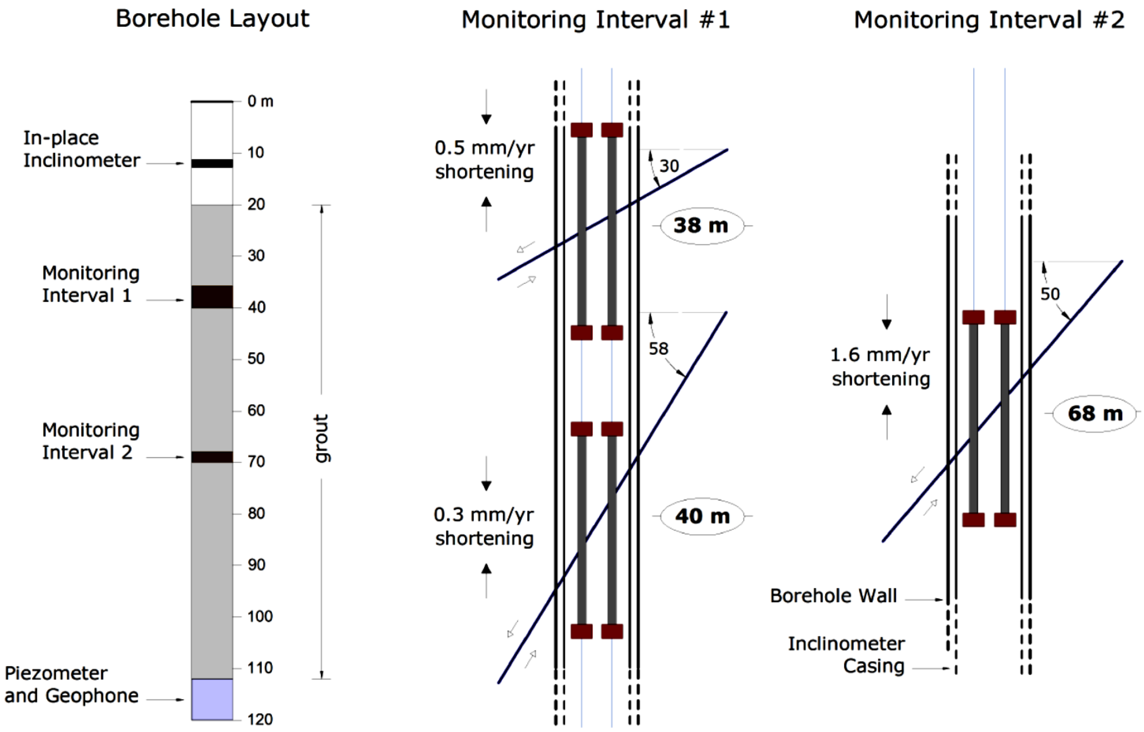

Fig. 4.13.2: Illustration of optical sensor installation, operating as crackmeter in boreholes (Moore, J.R. el al., 2010)

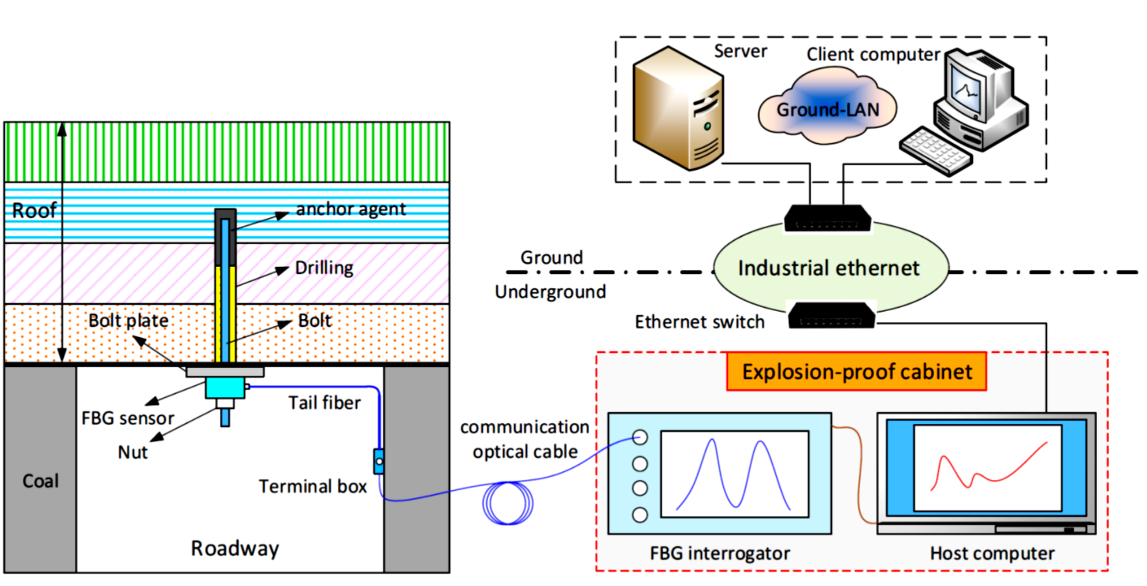

Fig. 4.13.3: Illustration of anchor force monitoring using FBG sensors (Liang & Fang, 2018)

Wu et al. (2022) applied a FGB system to monitor the deformation of a masonry retaining wall colonized by trees. Due to extreme weather conditions (typhoons or heavy rainfall) slope failure may occur. Therefore, the deformation of the retaining wall and the tress behind is monitored and a warning system gives alarm in case of any critical movement.

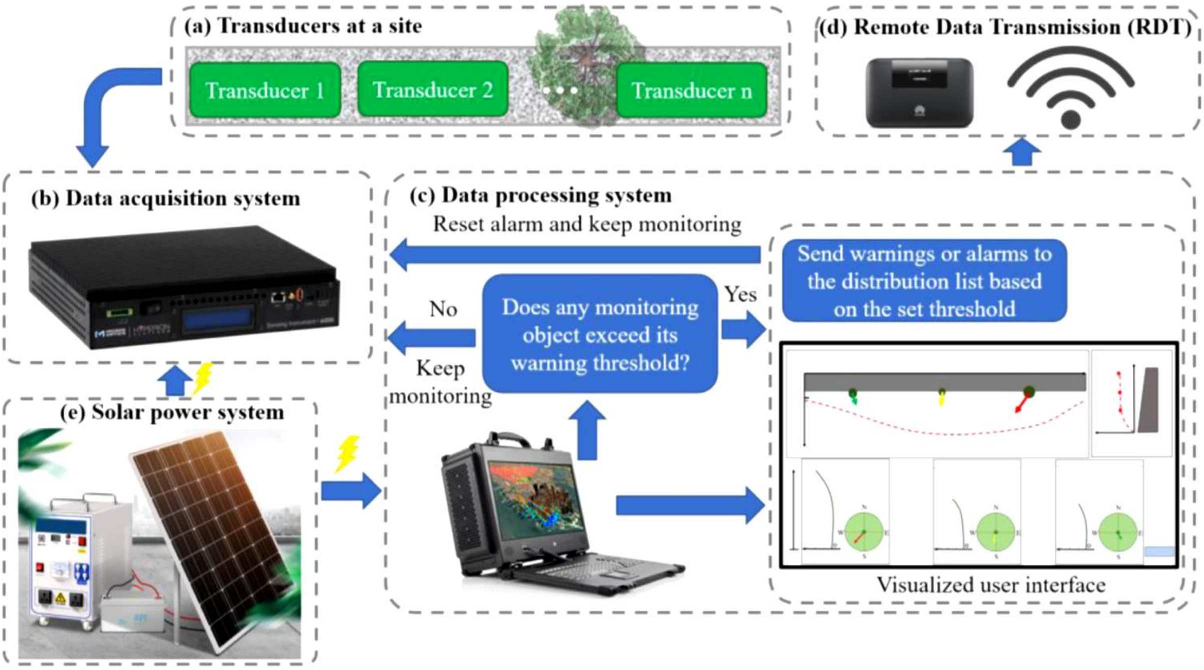

Fig. 4.13.4: Monitoring and warning system using FBG sensors (Wu et al., 2022)

Grunicke et al. (2021) demonstrate the application of distributed fibre optic sensing (DFOS) for long-term monitoring of not inspectable tunnel linings in respect to cracking. They show that cracks can be detected already at crack width of < 0.1 mm. The spatial resolution, important to localize cracks, can reach 10 mm or even less. DFOS uses either Rayleigh scattering or Brillouin scattering.

Fibre optical systems can – depending on material and measuring principle - measure temperatures up to about 600 °C and deformations up to 30 mm/m. The spatial resolution of DFOS is in the mm-range (Rayleigh scattering) or the cm-range (Brillouin scattering). The spatial resolution of FGB is typically in the cm-range. DFOS on the basis or Rayleigh scattering can be used up to measuring lengths of about 20 m, where Brillouin scattering allows lengths up to about 5 km.

Fig. 4.13.5 documents pros and cons of different sensing systems for deformation monitoring with emphasis on fibre optical systems.

Fig. 4.13.6 shows different types of optical fibres and cables. Fig. 4.13.7 provides some data / parameters of commercial distributed strain sensing. Fig. 4.13.8 illustrates typical fibre optical measurement arrangements.

Comparison of monitoring systems based on different sensing techniques.

Method	Pros	Cons	Application
Monitoring system based on FBG technology	Quasi-distributed sensing, real-time monitoring, suitable for both static and dynamic monitoring, suitable for the measurement under extreme weather, easy for multiplexing, high accuracy and stability	Costly, fragile if no protection, strain measurement within 1%	Monitoring of structures, geohazards, earth structures, and dynamic behavior trees (Pei et al., 2013; Hong et al., 2016; Zhu et al., 2017a,b; Li et al., 2020; Wu et al., 2021)
Monitoring system based on distributed fiber optic sensing (DFOS) technology	Fully distributed sensing, real-time monitoring, good for quasi-static or low-frequency application, suitable for the measurement under extreme weathers	Not efficient for long-distance dynamic monitoring (Cazzulani et al., 2021), strain measurement within 1%	Monitoring of pipes, slopes, landslides and earth structures (Ni et al., 2018; Zhang et al., 2018, 2020, 2021; Feng et al., 2019)
Monitoring system based on prisms	Real-time monitoring, suitable for both static and dynamic monitoring, high accuracy	Discrete sensing, complicated setup, small measurement range	Monitoring of sway motion of trees (Hassinen et al., 1998)
Monitoring system based on laser-related techniques	Real-time monitoring, suitable for both static and dynamic monitoring, high accuracy	Not suitable for typhoon conditions, discrete sensing	Structural health monitoring and natural frequency measurement of trees (Baker, 1997; Staszewski et al., 2004; Park et al., 2007)
Monitoring system based on conventional electronic sensors	Real-time monitoring, suitable for both static and dynamic monitoring, economical	Not suitable for thunderstorm or heavy rain conditions, discrete sensing, hysteresis and sensor drift	Monitoring of structures, earth structures (Admassu et al., 2019; Katsuda et al., 2019)

Fig. 4.13.5: Pros and cons of different deformation monitoring systems (Wu et al., 2022)

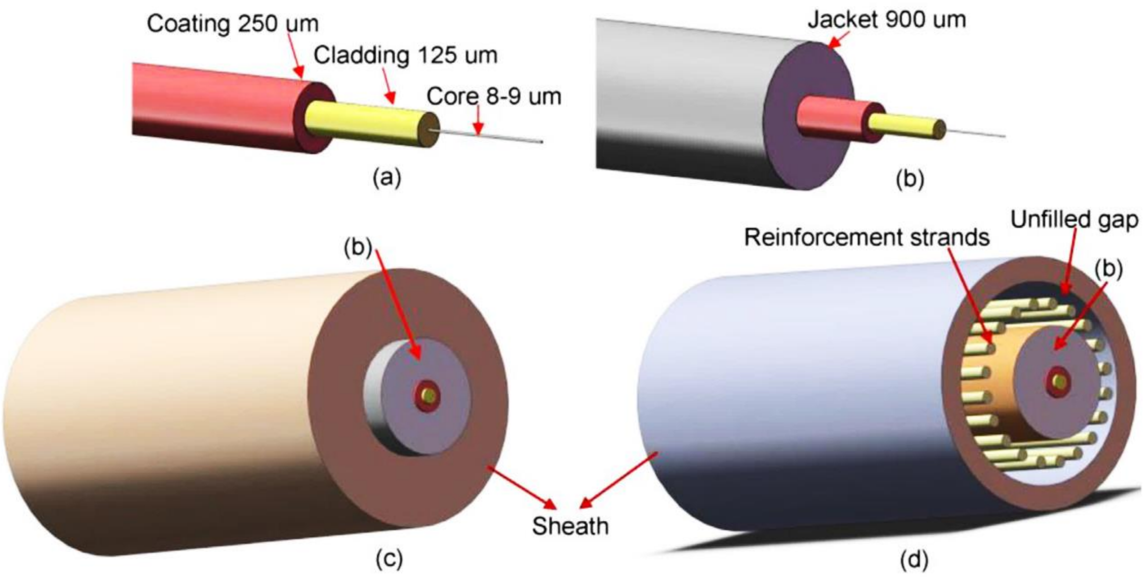

Fig. 4.13.6.: Typical structures of optical fibres and cables (Zhang et al., 2024)

Overview of typical interrogator systems for distributed strain sensing.

Manufacturer	Interrogator Type	Working Principle	Key System Parameter Specifications				
			Spatial resolution* (m)	Maximum sensing distance (km)	Sampling distance (m)	Strain range**and accuracy*	Temperature range** and accuracy*
Smartec, Switzerland (Smartec, 2022)	DiTeST	BOTDA BOTDR	1–20 1.5–20	60 45	0.25	>5% 2×10^{-6}	−150 to 1000 °C 0.1 °C
fibrisTerre, Germany (FibrisTerre, 2022)	fTB 5020/ 2505	BOFDA	0.2–2.5	80	0.05	−3% to 4% 2×10^{-6}	0.1 °C
		BOFDR	1.5	25		−0.2% to 4% 2×10^{-5}	1 °C
Neubrex, Japan (Neubrex, 2022)	NBX-6050A	BOTDA	0.05–1	25	0.01	−3% to 4% 7.5×10^{-6}	0.35 °C
	NBX-6055A	BOTDA	0.05–1	25	0.01	−3% to 4% 7×10^{-6}	0.3 °C
CECT, China (Ceyear, 2023)	AV6419	BOTDR	1	80	0.05	±1.5% 1×10^{-5}	
OZ Optics, Canada (OZ Optics, 2022)	DSTS	BOTDA	0.1–50	160	0.05	−3% to 4% 2×10^{-6}	−270 to 2100 °C 0.1 °C
		BOTDR	1–80	70		−0.2% to 1% 1.6×10^{-5}	−100 to 500 °C 0.8 °C
Luna Innovations Inc., USA (Luna, 2022)	OBR4600/ ODiSi 610x	OFDR	0.00065 −0.01	0.01–0.2****	0.00065 −0.01	±1.5% 1×10^{-6}***	−40 to 200 °C 0.5 °C
Mega-sense Inc., China (Mega-sense, 2022)	OSI–S/OSI –C	OFDR	0.001–0.01	0.05–0.1****	0.001–0.01	±1.2% 1×10^{-6}***	−200 to 1200 °C 0.1 °C

Fig. 4.13.7: Typical parameters of commercial distribution sensing devices (Zhang et al, 2024)

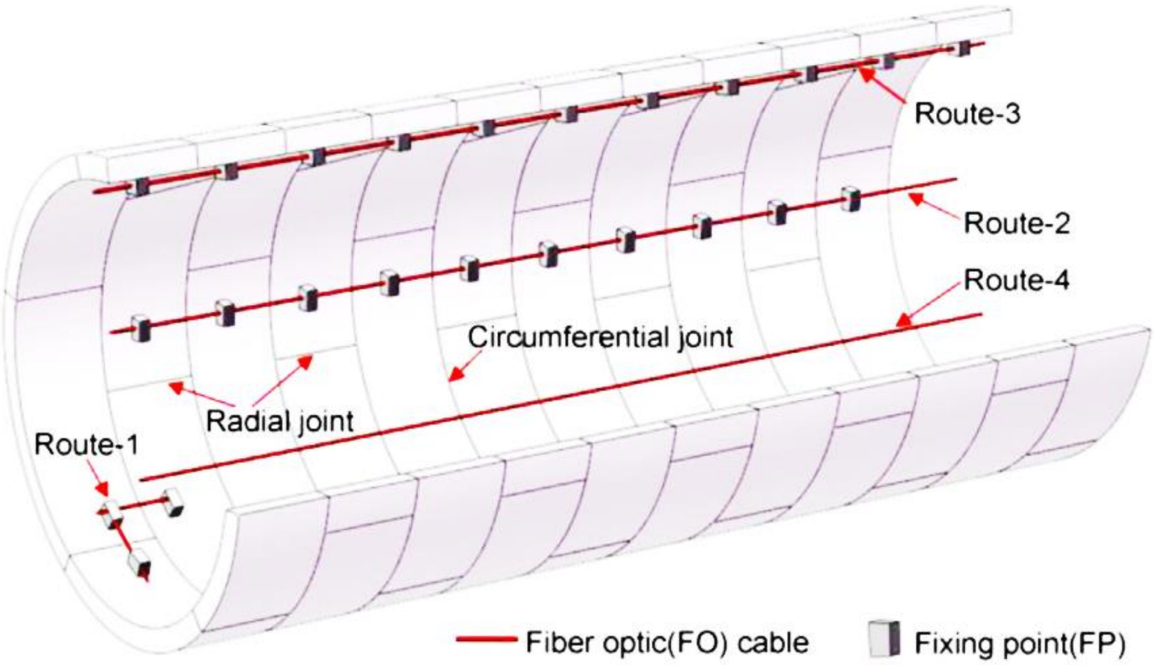

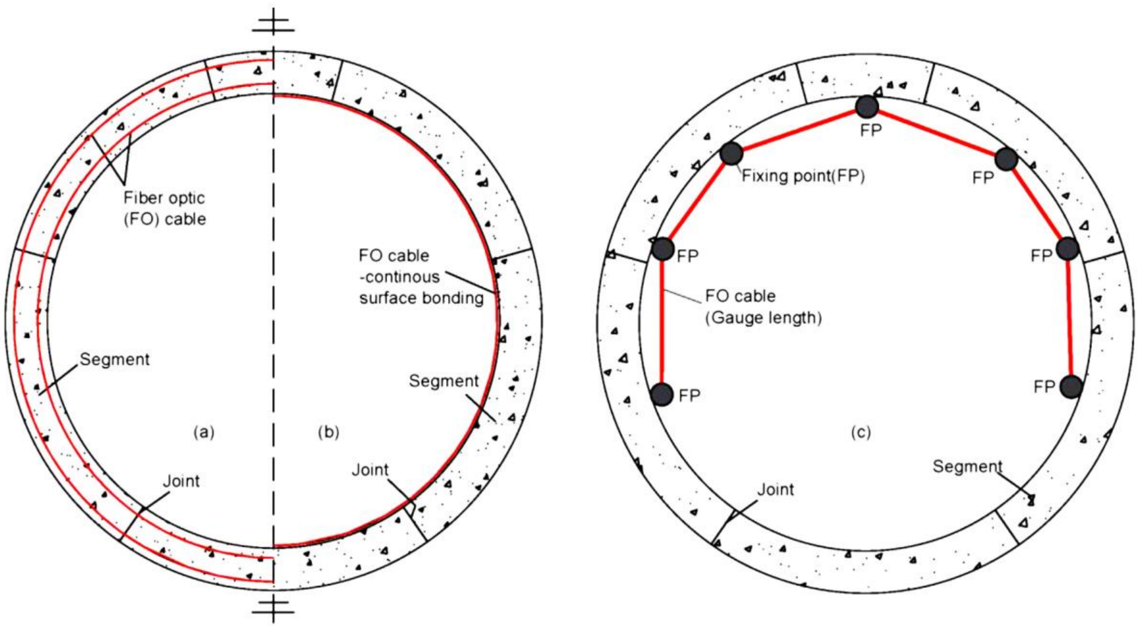

Fig. 4.13.8: Typical installation fibre optics installation arrangements fur tunnels (Zhang et al, 2024)

4.14 Time-domain reflectometers (TDR)

TDR measures reflections along a conductor, for instance along a cable and works like a radar (see for instance: Hernandez-Meija, 2016). The incidence signal is reflected at the end of the conductor as well as at disturbances in between. Based on the travel time difference between reflected pulses and difference in amplitude and shape between incidence and reflected signal the characteristic impedance of the trace is determined. The travel time differences allow the determination of the location of the disturbance and the shape difference allows to classify the type of disturbance.

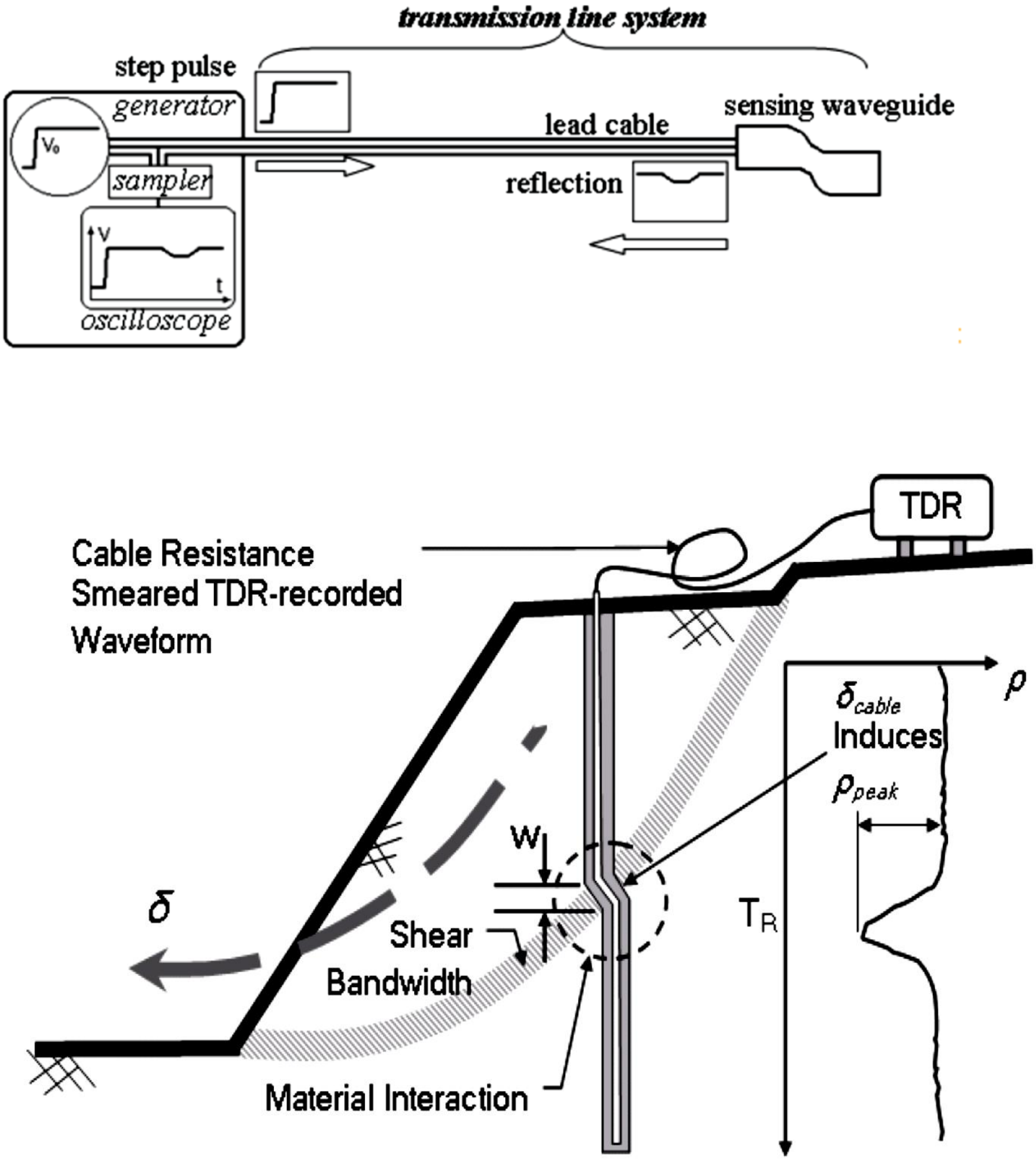

Fig. 4.14.1: TDR measurements: above: principle, below: application for slope monitoring (Lin, 2009)

4.15 Plump wire measuring systems

Plump wire measuring systems are typically applied for water dams (barrages) and allow to measure horizontal displacements and bending with high accuracy. Fig. 4.15.1 and 4.15.2 show two common types of installation. Fig. 4.15.3 shows a corresponding optical position measuring device. Resolution is about 0.01 mm and accuracy about 0.1 mm.

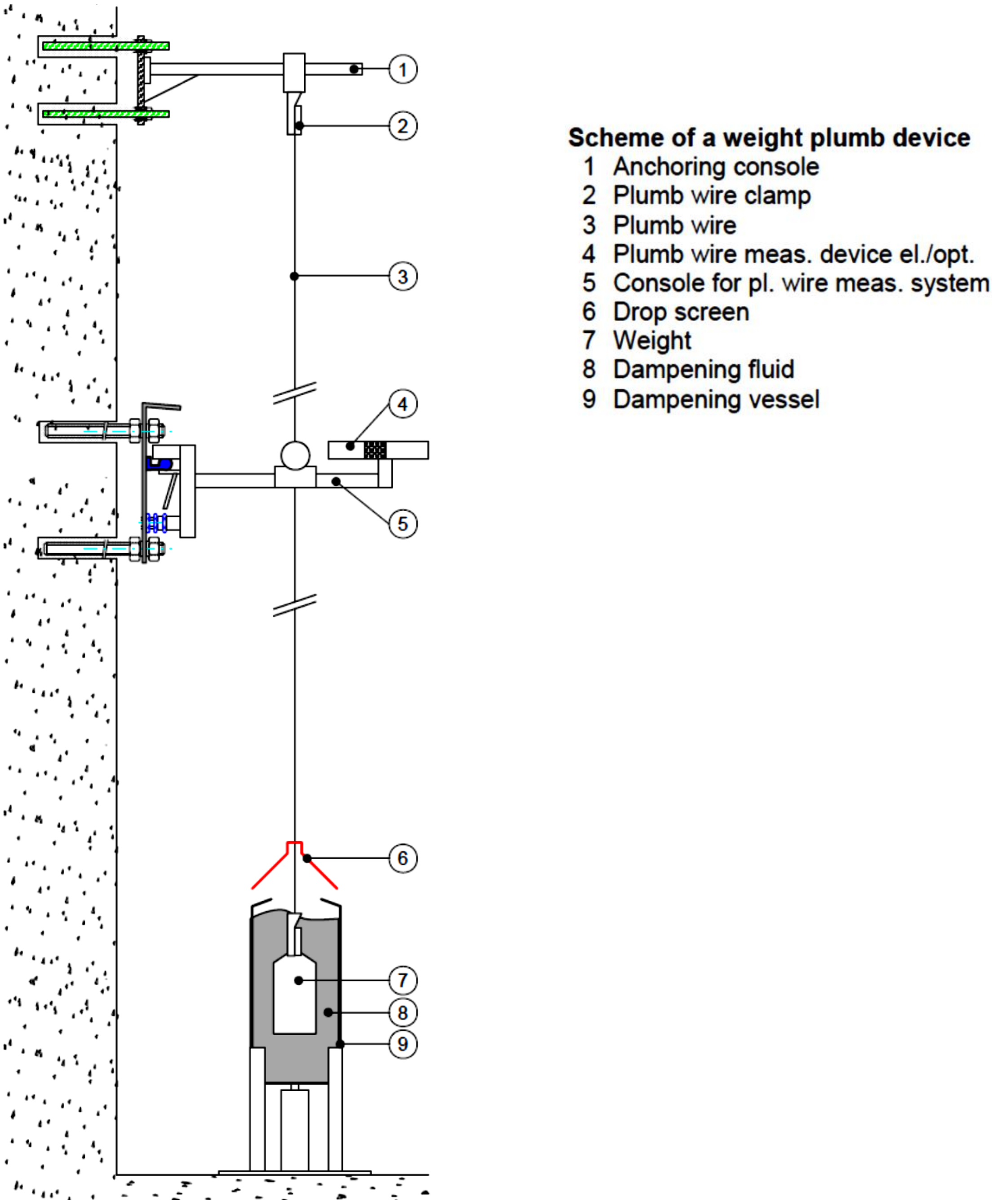

Fig. 4.15.1: Weight plump measuring system (Glötzl, company material, 2022)

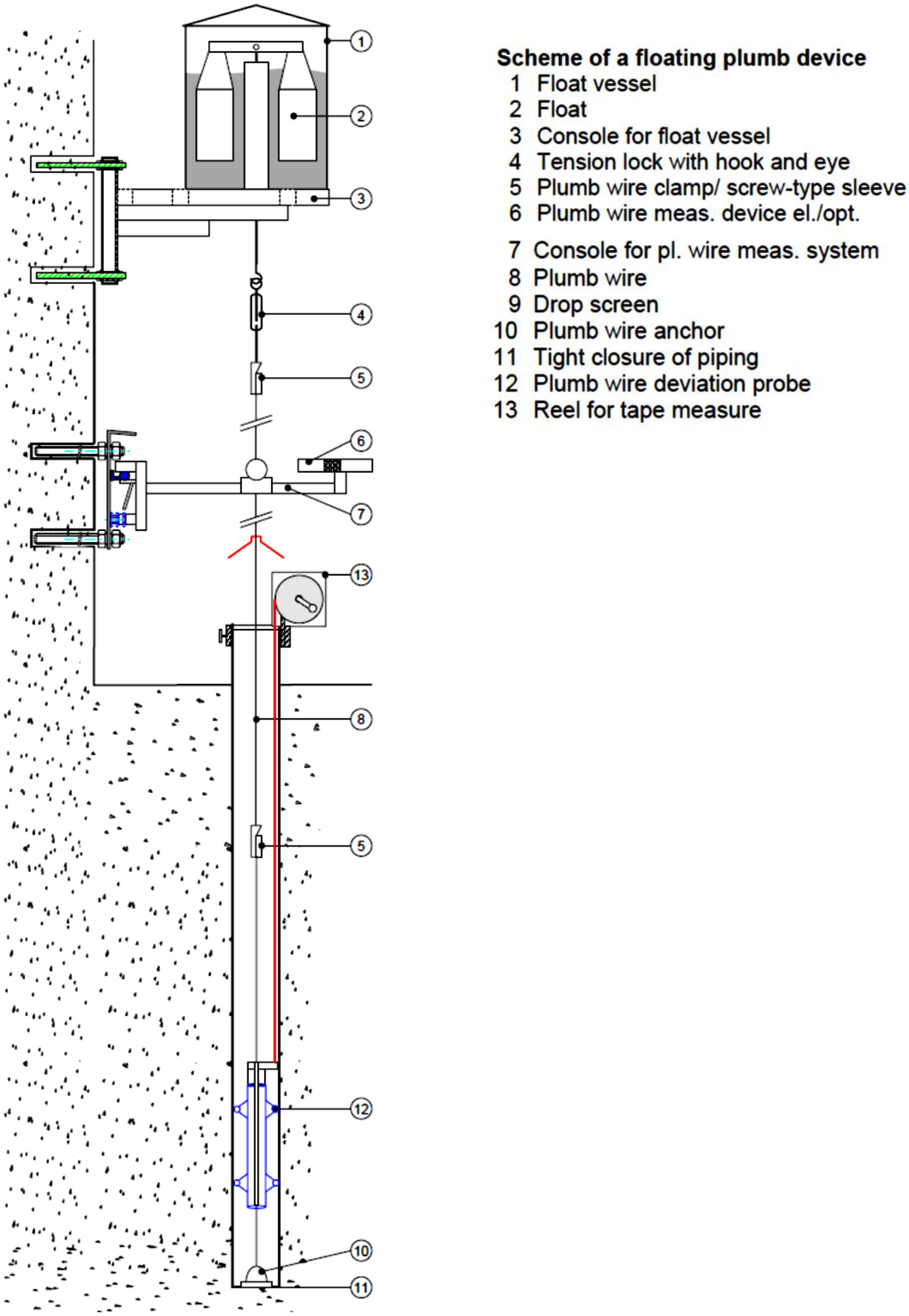

Fig. 4.15.1: Floating plump measuring system (Glötzl, company material, 2022)

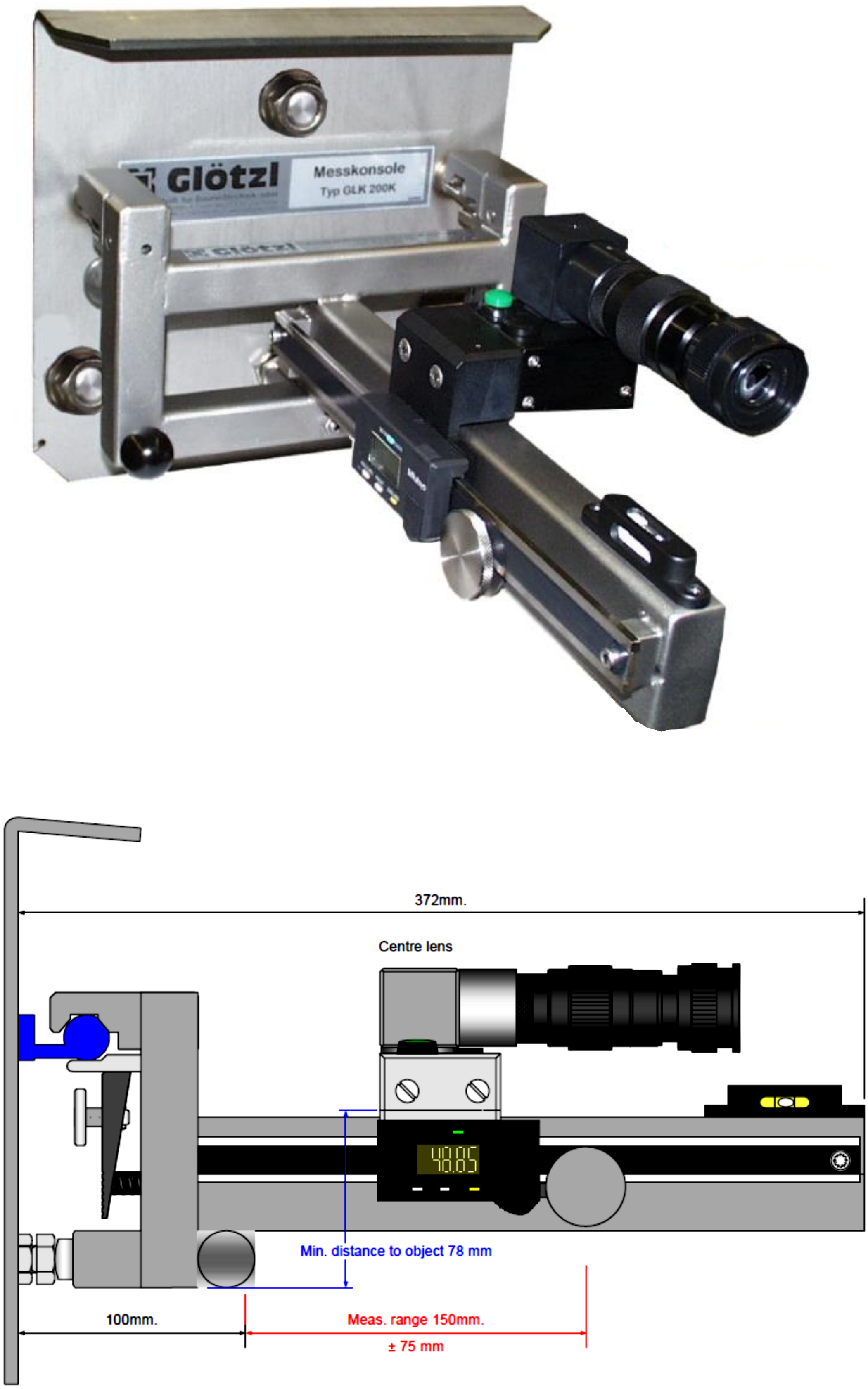

Fig. 4.15.3: Alignment wire position measuring device (Glötzl, company material, 2022)

4.16 Measuring anchor

A measuring anchor is a combination of an extensometer and an anchor. Inside a hollow anchor road several fixed measuring rods are placed. With a dial gauge the movement of the measuring roads is determined. This system replaces an anchor and allows in addition to get information about the load distribution along the anchor length with low costs. Fig. 4.16.1 shows the set-up of a measuring anchor with 4 measuring rods. Measuring accuracy is about 0.01 mm.

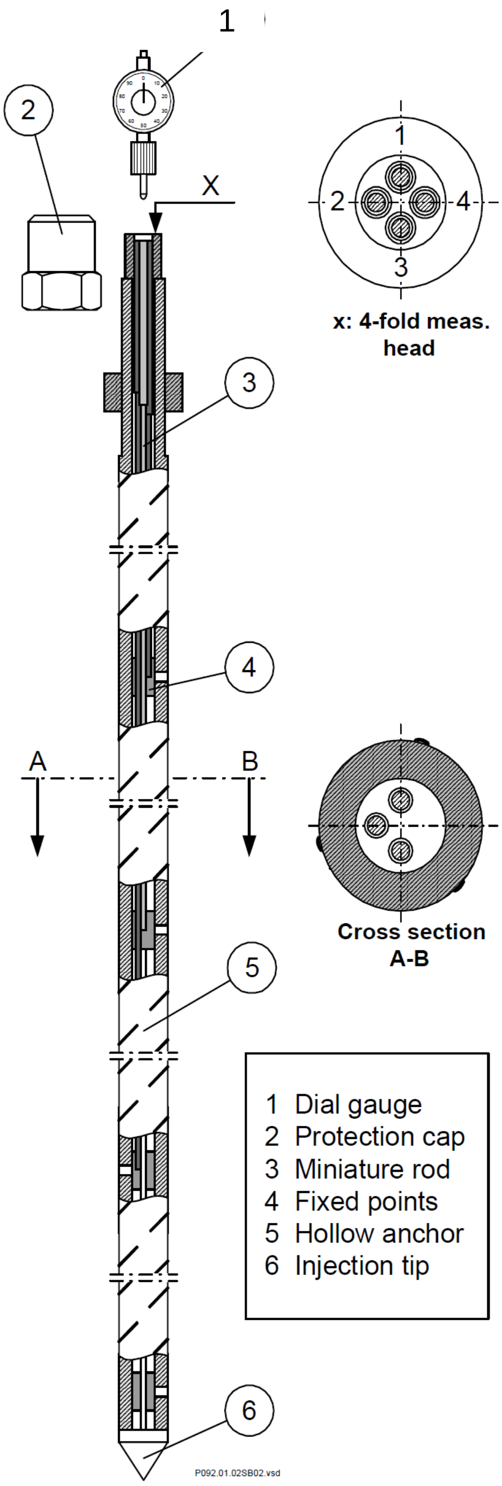

Fig. 4.16.1: Measuring anchor (Glötzl, company material, 2022)

5 Examples

Radoncic et al. (2021) present a nice example for a complex geotechnical monitoring system for a near-surface underground tunnel construction (connection of airport in Montreal with subway grid, see Fig. 5.1). Main concern of the construction was to minimize surface movements and to guarantee safety.

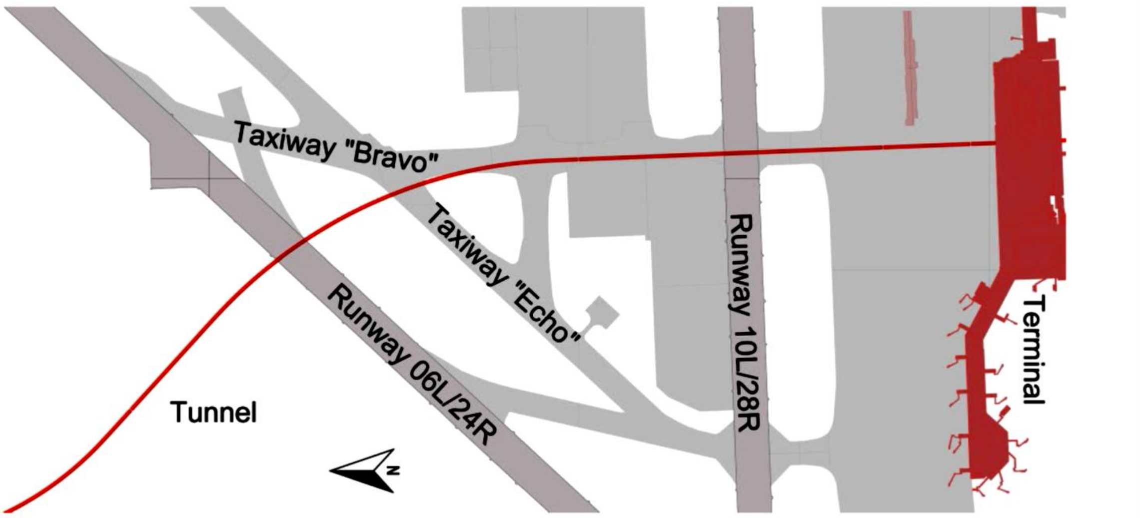

Fig. 5.1: Illustration of tunnel project: red line indicates tunnel route (Radoncic et al., 2021)

The complex monitoring system comprises the following items:

- 3D tachymeter measurements at the ground surface and inside the tunnel
- Chain inclinometer
- Inclinometer
- Multiple extensometers
- Strain gauges in precast concrete segments (tunnel lining)
- InSAR monitoring

Fig. 5.2 illustrates the installation of the above mentioned monitoring systems. All devices are accessed via a civil GSM band.

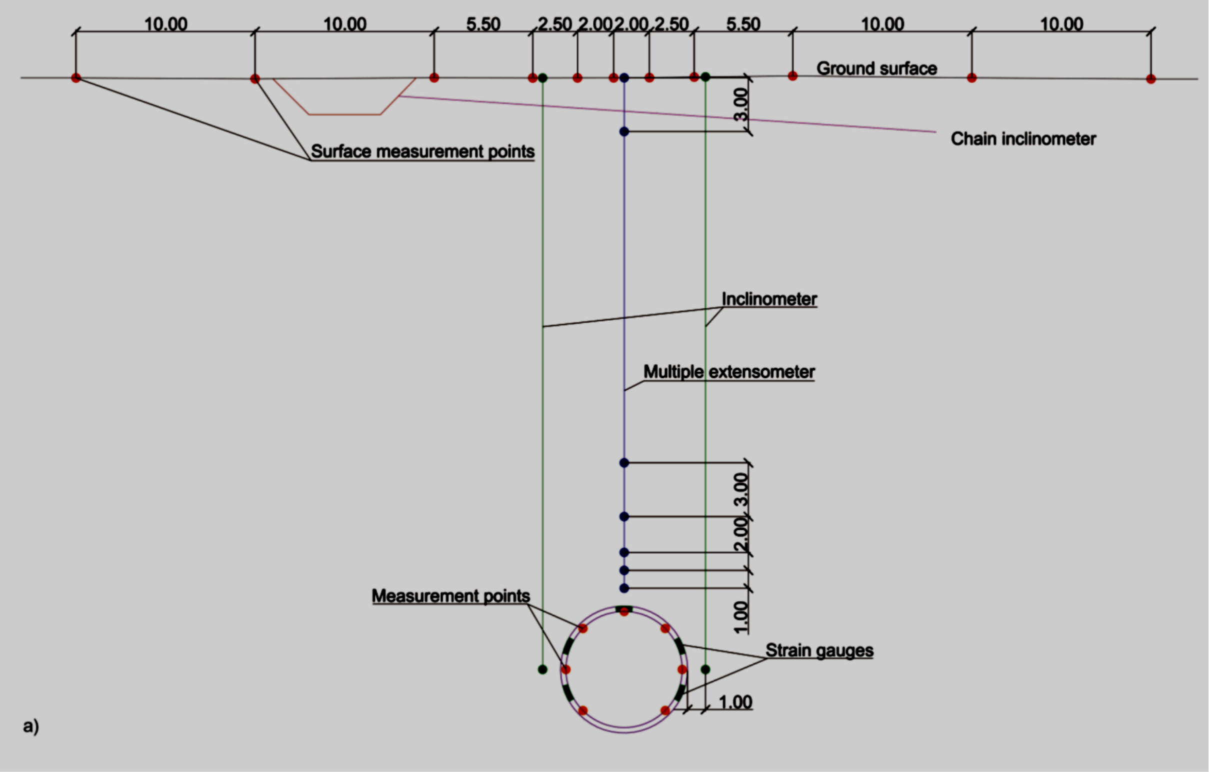
10.00
10.00
5.50
2.50
2.00
2.00
2.50
5.50
10.00
10.00
Ground surface
3.00
Chain inclinometer
Surface measurement points
Inclinometer
Multiple extensometer
3.00
2.00
1.00
Measurement points
Strain gauges
1.00
a)

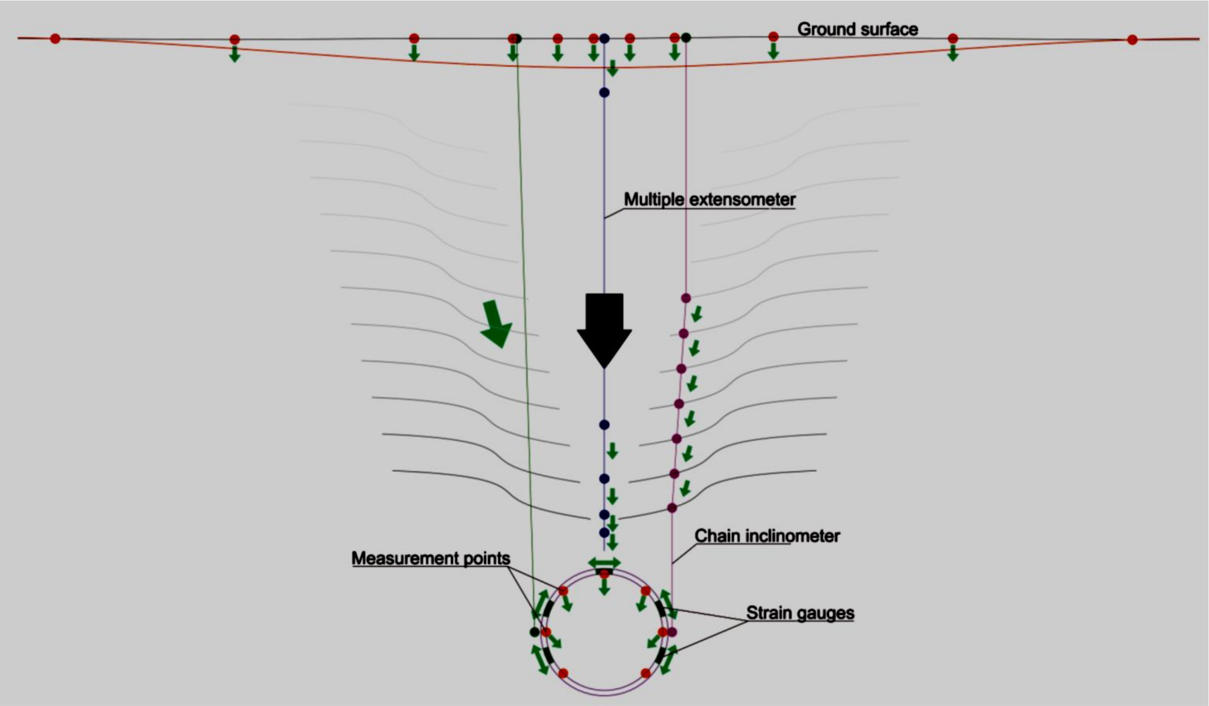
Ground surface
Multiple extensometer
Chain inclinometer
Measurement points
Strain gauges

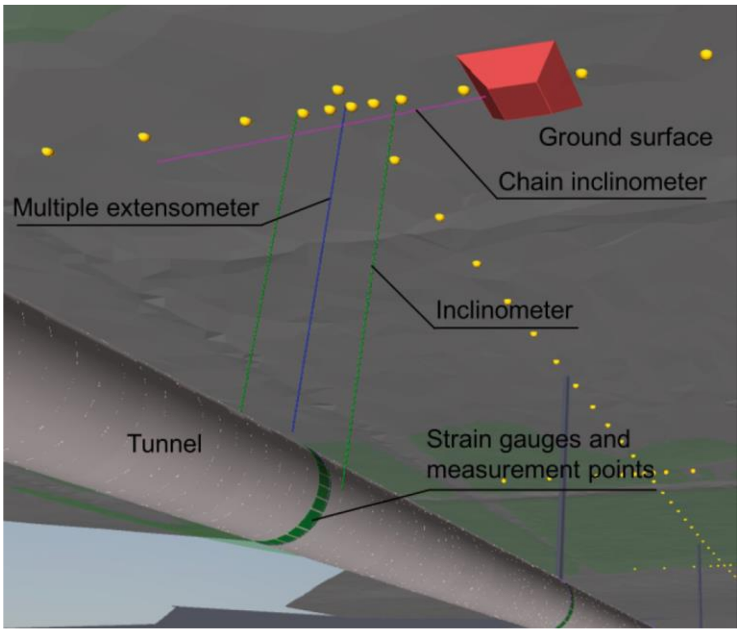

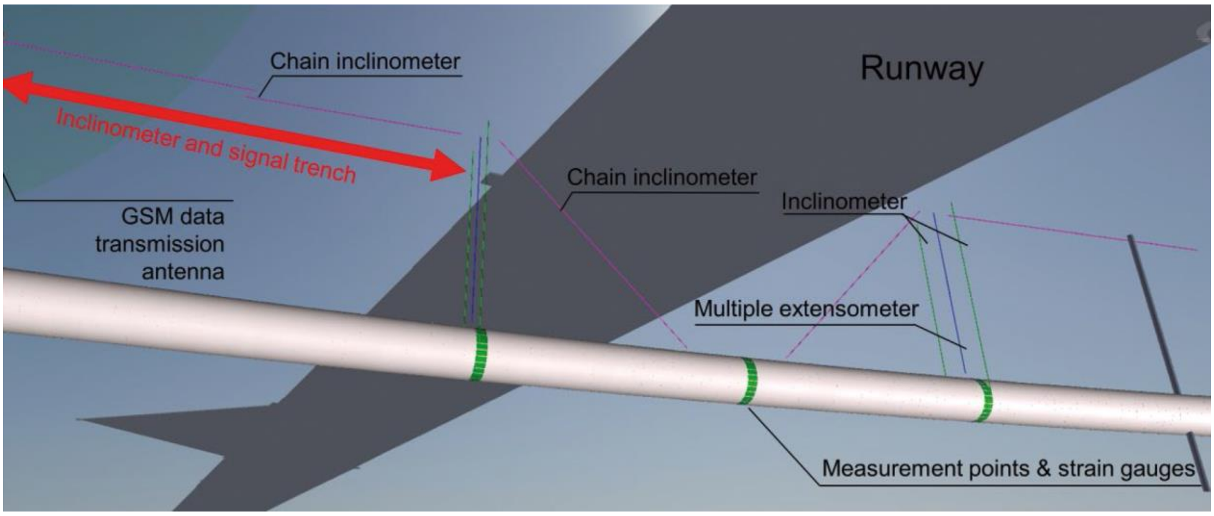

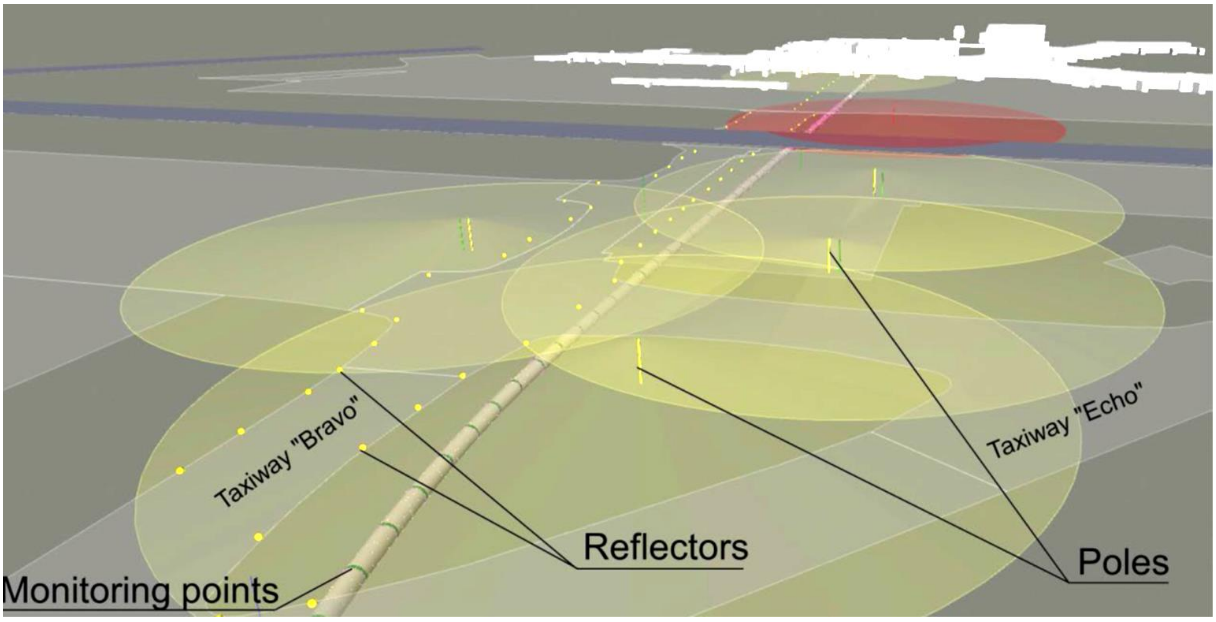

Fig. 5.2: Illustration of installed monitoring systems (Radoncic et al., 2021)

Another nice example is documented by NAGRA (2019: A full-scale emplacement experiment incl. heating performed at the URL Mont Terri. Fibre-optical sensing was used to measure the temperature evolution in a backfilled tunnel with emplaced heater systems (see Fig. 5.3). The mechanical behaviour during the experiment was observed via convergence measurements and 4-point-extensometers (see Fig. 5.4). During the experiment also inclinometer, pressure cells, thermocouple temperature sensors, humidity sensors, anemometers, extensometers, AE sensors and few more special sensors were applied.

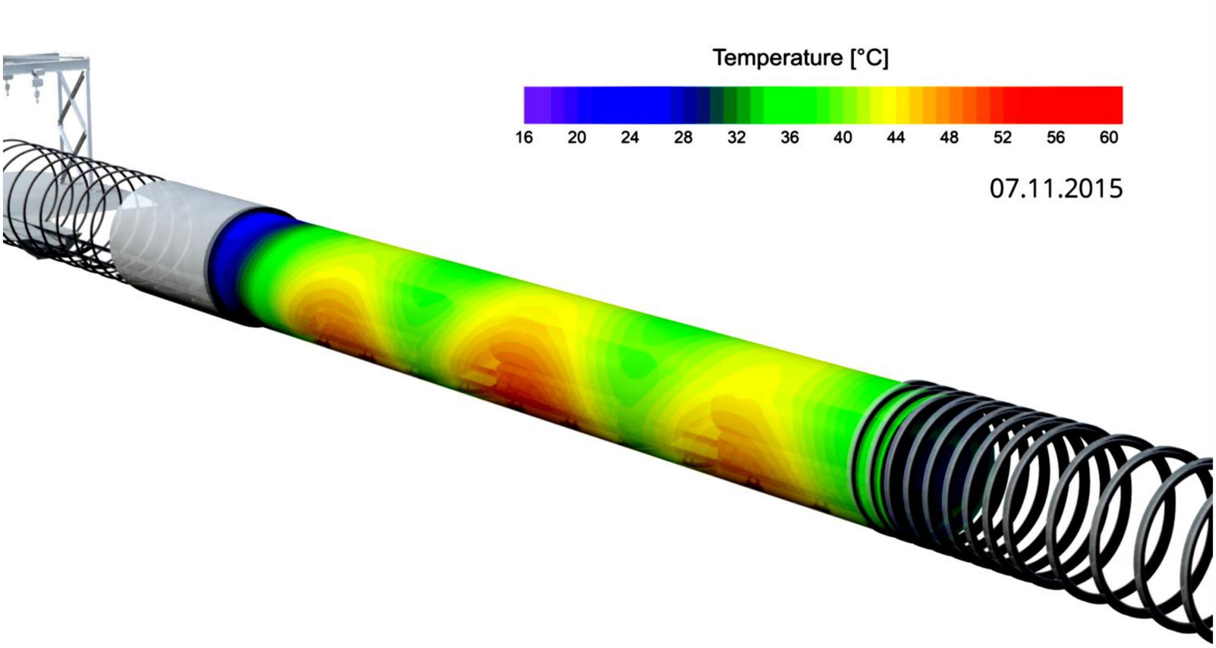

Fig. 5.3: Tunnel wall temperature measured by fibre-optic distributed sensing (Nagra 2019)

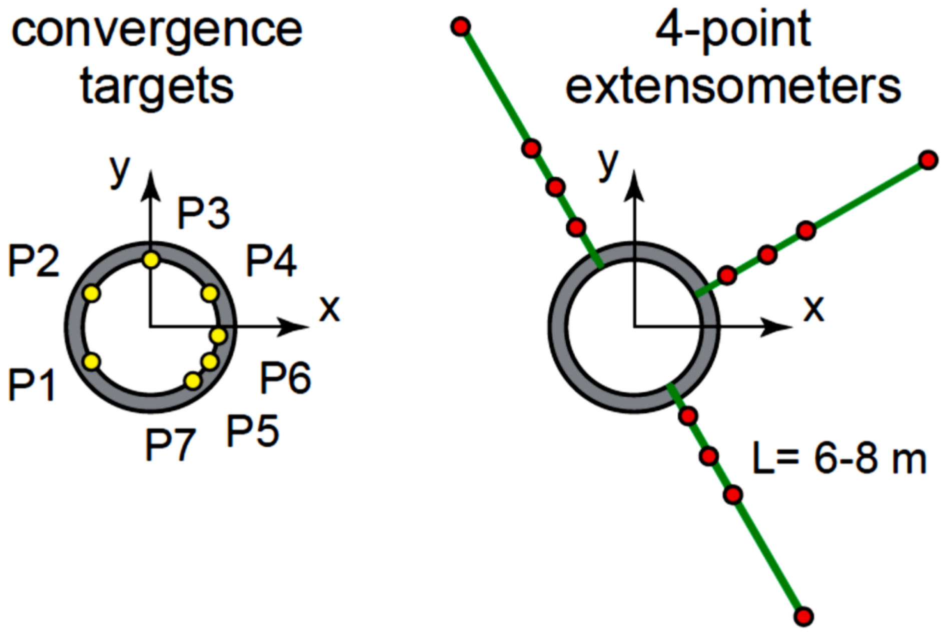

Fig. 5.4: Layout of convergence and dilatometer measurements (Nagra 2019)

Another example is the in-situ shear test as illustrated in Fig. 5.5. Within a test chamber a rock block (edge length up to several meters) is created. Normal and shear forces are stepwise or continuously increased via hydraulic props until the rock block is sheared off. The shear plane is typically a fracture or another discontinuity. Normal and shear forces (stresses) are measured as well as horizontal and vertical displacement. Such tests are performed to determine large scale in-situ strength (e.g. cohesion, friction and dilation angle) and stiffness (normal and shear stiffness) of discontinuities.

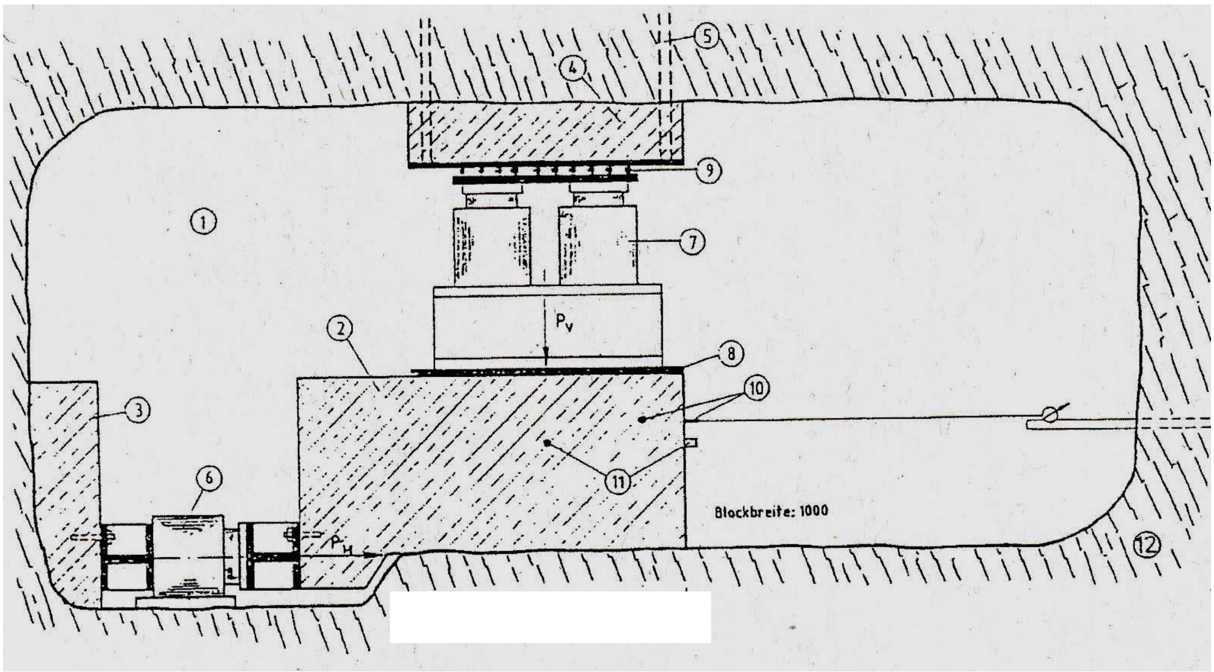

Fig. 5.5: In-situ shear test (Biewald et al. 1997): (1) test chamber, (2) rock block, (3) horizontal abutment, (4) vertical abutment, (5) anchors for abutment fixation, (6) hydraulic prop for horizontal force, (7) hydraulic props for vertical force, (8) load distribution plate, (9) roller bearing, (10, 11) displacement measurement systems, (12) rock mass

Radioactive waste disposal place particular high demands on monitoring. Therefore, a lot of different sensors are used for the measurement and supervision of different parameters. Special attention is paid to redundancy, robustness and longevity.

Fig. 5.6 shows a potential monitoring system for nuclear waste cell. Fig. 5.7 shows a gallery with installed monitoring systems comprising fiber optic sensors, extensometers, pressure cells, pore water pressure sensors, displacement sensors, permeability sensors and TDR sensor for water content measurement.

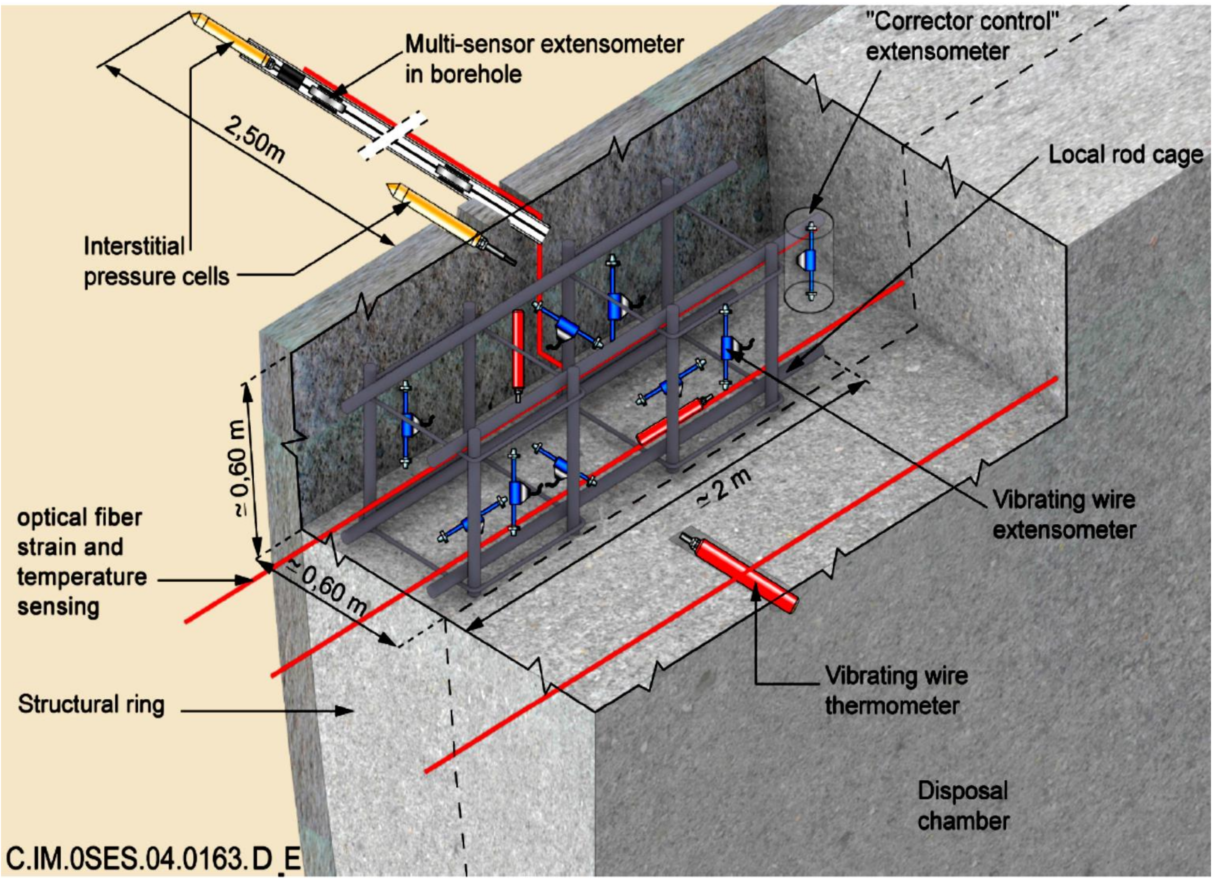

Fig. 5.6: Envisioned monitoring system for a nuclear waste repository cell (Delepine-Lesoille, 2017)

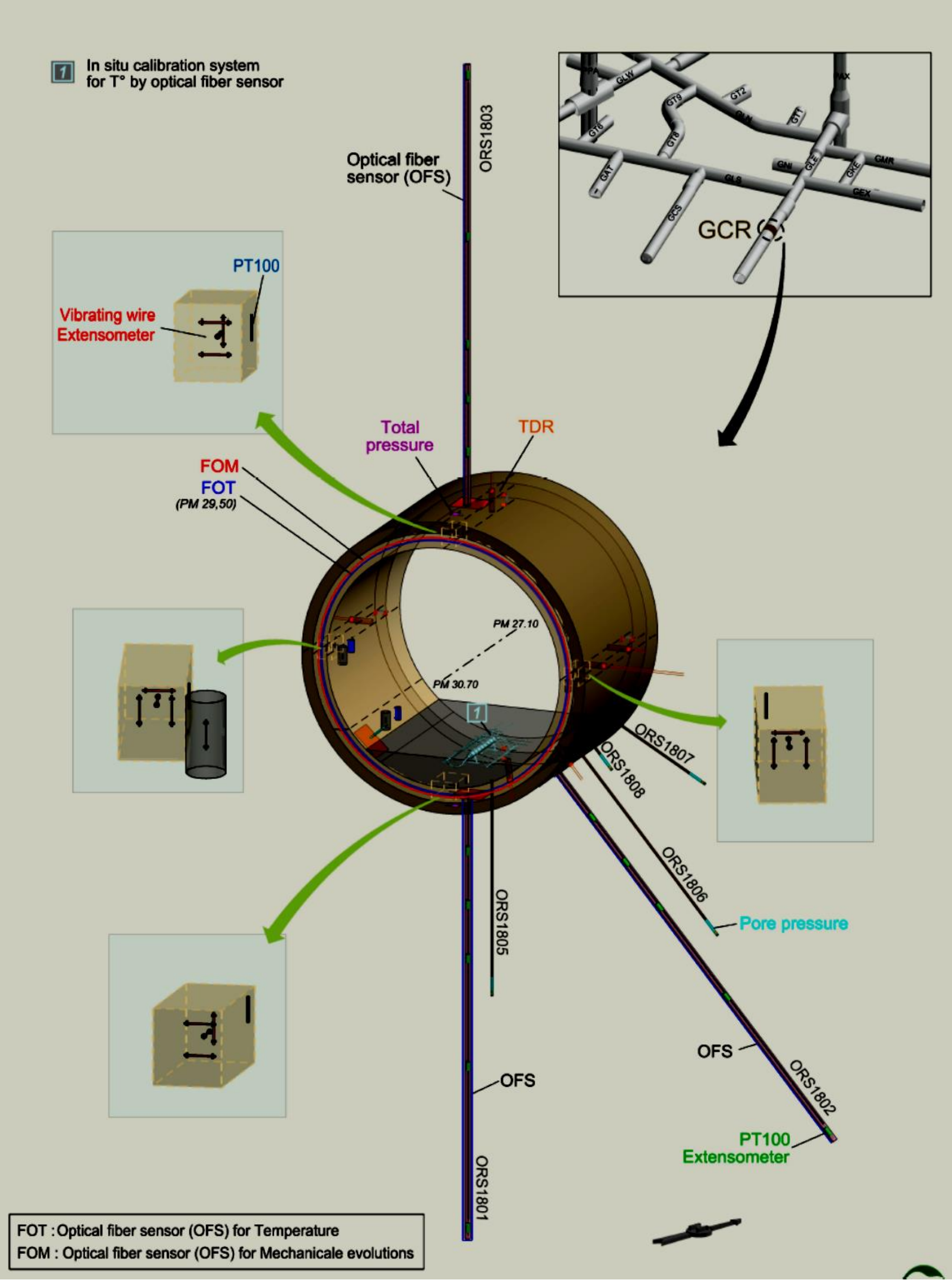

Fig. 5.7: Monitoring section in the GCR gallery (Delepine-Lesoille, 2017)

6 References

Aghaziri, A, Tannat, D.D., Martin, D. (2012): Characterizing rock mass deformation mechanisms during plate load tests at the Bakhtiary dam project, *Int. J. Rock Mech. Min. Sci.*, 49: 1-11

ASTM D 4403-84 (2005, reapproved): Standard practice for extensometers used in rock

ASTM D 4394-08 (2008): Standard test method for determining the in situ modulus of deformation or rock mass using rigid plate testing method

Biewald, W. et al. (1997): Die Talsperre Leibis/Lichte im Thüringer Schiefergebirge aus ingenieurgeologischer Sicht, Geowiss. Mitt. Thüringen, 5: 235-278

Delepine-Lesoille, S. et al. (2017): France's state of the art of distributed optical fibre sensors qualified for the monitoring of the French underground repository for high level and intermediate level long lived radioactive wastes, Sensors, 17: 1377

Eberhard, E. & Stead, D. (2011): Geotechnical Instrumentation, in: SME Mining Engineering Handbook (ed.: Darling, P.), *Soc. Mining Metallurgy*, 551-571

Franklin, J. (1980): Suggested methods for pressure monitoring using hydraulic cells, *Int. J. Rock Mech. Min. Sci.*, 17(2): 117-127

Golser, J. & Steiner, W. (2021): International and european standards for geotchnical monitoring and installation, Geomechanics and Tunneling, 14(1): 63-77

Goodman, R.E. (1968): Measurement of rock deformability in boreholes, ARMA-68-0523

Grunicke, U.H. et al. (2021): Long-term monitoring of visually not inspectable tunnel linings using fibre optic sensing, Geomechanics and Tunneling, 14(1): 19-32

Henzinger, M.R. (2018): Fibre-optic supported measurement methods for monitoring rock pressure, Geomechanics and Tunneling, 11(3): 251-263

Hernandez-Meija, J.C. (2016): Time domain reflectometry (TDR), Cable diagnostic initiative, phase II, chapter 4, Georgia Tech research Corp.

Janeras, M.; Jara, J. A.; López, F.; Marturià, J.; Royán, M. J.; Vilaplana, J. M. et al. (2015): Using several monitoring techniques to measure the rock mass deformation in the Montserrat Massif, *IOP Conf. Ser.: Earth Environ. Sci.* 26, p 12030.

Kavur, B., Stambuk Cvitanovic, N., Hrzenjak, P. (2015): Comparison between plate jacking and large flat jack test results of rock mass deformation modulus, *Int. J. Rock. Mech. Min. Sci.*, 73: 102-114

Konietzky, H.; Lorenz, K.; Witter, W., (2004a): Simulation of landslide movements based on a multidisciplinary approach, *Felsbau*, 22(2): 23-32

Konietzky, H.; Lorenz, K.; Stötzner, U., (2004b): Die Standsicherheit von Stauraum-hängen unter extremen Niederschlagsszenarien: Rückrechnungen und Prognosen, *Veröffentl. Institut für Geotechnik*, TU Bergakademie Freiberg, 2004(4): 201-214

Liang, M. & Fang, X. (2018): Application of fiber bragg grating sensing technology for bolt force status monitoring in roadways, Appl. Sci. 8: 107

Li, S.J. et al. (2013): ISRM suggested method for measuring rock mass displacement using sliding micrometer, *Rock Mech Rock Eng*, 46: 645-653

Lin, C.-P. (2009): geotechnical sensing by TDR: a slope monitoring system example, Proc. 9. Int. offshore and polar conference, 242-245

Moore, J.R. (2010): Rockslide deformation monitoring with fibre optic strain sensors, Nat. Hazards Earth Syst. Sci. 10: 191-201

Nagra (2019): Implementation of the full-scale emplacement experiment at Mont Terri, NTB 15-02

ISRM (1979): Suggested methods for determining the in situ deformability of rock, *Int. J. Rock Mech. Min. Sci.*, 16: 195-214

Paul, A., Walter, F. (2004): Empfehlung Nr. 19 des AK 3.3 Versuchstechnik Fels der DGGT: Messung der Spannungsänderung im Fels und an Felsbauwerken mit Druckkissen, *Bautechnik*, 81(8): 639-647

Radoncic, N. et al. (2021): Design a state-of-the-art monitoring system in challenging operation conditions, Geomechanics and Tunneling, 14(1): 54-62

Tang, B. & Cheng, H. (2018): Application of distributed optical fibre sensing technology in surrounding rock reock deformation control of TBM-excavated cola mine roadway, Journal of Sensors, ID 8010746

Temnykh, A. (1997): Vibrating wire field-measuring technique, *Nuclear Instruments and Methods in Physics Research A*, 399: 185-194

Thüringer Fernwasserversorgung (2007): Hangbewegung Gabel – Ein Beitrag zur Talsperrensicherheit, 51 p. (http://www.thueringer-fernwasser.de/downloads.html)

USBR 6515 (2009): Procedure for using piezometers to monitor water pressure in rock mass

Wu, P. et al. (2022): Development of a monitoring and warning system based on optical fiber sensing technology for masonry retaining walls and trees, Journal of Rock Mechanics and Geotechnical Engineering, 14: 1064-1076

Wyllie, D.C. (2017): Rock slope engineering, CRC Press, 568 p.

Yow, J.L. (2014): Borehole dilatometer testing for rock engineering, in: Hudson (ed.): *Comprehensive Rock Engineering*, Pergamon Press, Vol. 3, 671-681

Zalesky, M. et al. (2007): Dilatometer tests in deep boreholes in investigation for Brenner base tunnel, *Underground Space - the 4th Dimension of Metropolis* (ed. Bartak et al.), Taylor & Francis, ISBN 987-0-415-40807-3, 283-288

Zhang, X. et al. (2024): Distributed fiber optic sensors for tunnel monitoring: a state-of-the-art review, J. Rock Mech. Geotech. Eng., 16: 3841-3863